

**THE HIGGS BOSON AND RIGHT-HANDED  
NEUTRINOS IN SUPERSYMMETRIC MODELS**

**A Thesis Submitted to  
the Graduate School of Engineering and Sciences of  
İzmir Institute of Technology  
in Partial Fulfillment of the Requirements for the Degree of**

**MASTER OF SCIENCE**

**in Physics**

**by  
ÖZER ÖZDAL**

**July 2016  
İZMİR**

We approve the thesis of **ÖZER ÖZDAL**

**Examining Committee Members:**

---

**Prof. Dr. Durmuş Ali DEMİR**

Department of Physics, İzmir Institute of Technology

---

**Assist. Prof. Dr. Levent SELBUZ**

Department of Engineering Physics, Ankara University

---

**Assist. Prof. Dr. Fatih ERMAN**

Department of Physics, İzmir Institute of Technology

**22 July 2016**

---

**Prof. Dr. Durmuş Ali DEMİR**

Supervisor, Department of Physics,  
İzmir Institute of Technology

---

**Prof. Dr. R. Tuğrul SENGER**

Head of the Department of  
Physics

---

**Prof. Dr. Bilge KARAÇALI**

Dean of the Graduate School of  
Engineering and Sciences

## ACKNOWLEDGMENTS

I would like to thank my supervisor Prof. Dr. Durmuş Ali Demir for his great contribution. Our discussions about physics always made me excited and made me feel myself more and more productive in physics. He has always been willing to listen to any problem and to provide helpful suggestions. I am also extremely grateful to Dr. Cem Salih Ün for his great contribution, helpful guidance and his endless patience and support. He always encouraged me even when I removed all the data by mistake. I have learned a lot from him about the computational aspects of high energy physics. I was inspired from his knowledge and enthusiasm in physics during two years. He was more than a collaborator for me. I believe, I will always feel his brotherhood till the end of my life.

I would like to thank to the other members of my defence committee, Prof. Dr. Durmuş Ali Demir, Assist. Prof. Dr. Levent Selbuz and Assist. Prof. Dr. Fatih Erman for helpful comments and giving suggestions.

I also would like to thank to Kemal Gültekin, Hemza Azri, Ayşe Elçiboğa Kудay, Ulaş Özdemir and Zafer Kandemir for their friendship, support and their useful discussions about physics. We spent both useful and enjoyable coffee breaks together. I would also like to send my best regards to Assist. Prof. Dr. Zerrin Kırca and my friends Zafer Altın and Ali Cici from Uludağ University.

Finally, I would like to express my gratitude to my parents Ziyneti and Nail Özdal and my sister Özge Özdal for their endless support, encouragement, motivation and love during all my life.

This thesis study was supported by The Scientific and Research Council of Turkey (TUBITAK) project no:114F461. Therefore, I would like to thank TUBITAK for supporting me during my M.Sc. studies.

# ABSTRACT

## THE HIGGS BOSON AND RIGHT-HANDED NEUTRINOS IN SUPERSYMMETRIC MODELS

The results represented in this thesis are based on our work in [1], where the predictions on the mass spectrum and Higgs boson decays are investigated in the supersymmetric standard model extended by  $U(1)_{B-L}$  symmetry (BLSSM). The model requires two singlet Higgs fields, which are responsible for the radiative breaking of  $U(1)_{B-L}$  symmetry. Radiative breaking of  $U(1)_{B-L}$  symmetry yields right-handed neutrino of mass at the TeV scale. It predicts degenerate right-handed neutrino masses (1.7–2.2 TeV) as well as the right-handed sneutrinos of mass  $\lesssim 4$  TeV. The presence of right-handed neutrinos and sneutrinos trigger the baryon and lepton number violation processes, until they decouple from the Standard model particles. Besides, the model predicts rather heavy colored particles;  $m_{\tilde{t}}, m_{\tilde{b}} \gtrsim 1.5$  TeV, while  $m_{\tilde{\tau}} \gtrsim 100$  GeV and  $m_{\tilde{\chi}_1^\pm} \gtrsim 600$  GeV. Even though the implications on the SM-like Higgs boson are similar to minimal supersymmetric standard model (MSSM), BLSSM can predict another Higgs boson lighter than 150 GeV. We find that the second Higgs boson can be degenerate with the lightest CP-even Higgs boson of mass about 125 GeV and contribute to the Higgs decay into two photons. In addition, if it is not degenerate, it can provide a possible explanation for the excess in  $h \rightarrow 4l$  at the mass scale  $\sim 145$  GeV.

# ÖZET

## SÜPERSİMETRİK MODELLERDE HİGGS BOZON VE SAĞ-EL NÖTRİNOLAR

Bu tezde sunulan sonuçlar  $U(1)_{B-L}$  simetrisi ile genişletilmiş süpersimetrik standart modelde (BLSSM) kütle spektrumu ve Higgs bozonunun bozunmalarını araştırdığımız çalışmamıza dayanmaktadır [1]. Bu model ışınımsal  $U(1)_{B-L}$  simetrisini kırmaktan sorumlu iki adet tekil Higgs alanı içerir ve  $1.7 - 2.2$  TeV enerji skalasında dejenere sağ-el nötrino kütleleri ile kütlesi 4 TeV'den küçük snötrino öngörür. Sağ-elli nötrino ve snötrinoların varlığı baryon ve lepton sayısının korunumunun ihlal edildiği süreçleri bu parçacıklar Standart Model parçacıklarına ayrışına dek tetikler. Ayrıca, model oldukça ağır renkli parçacıklar;  $m_{\tilde{\tau}} \gtrsim 100$  GeV and  $m_{\tilde{\chi}_1^\pm} \gtrsim 600$  GeV iken  $m_{\tilde{t}}, m_{\tilde{b}} \gtrsim 1.5$  TeV, öngörür. Standart model benzeri Higgs bozon özellikleri minimal süpersimetrik standart modele çok benzese de, BLSSM 150 GeV'den hafif bir başka Higgs bozonu daha öngörür. Son olarak, bu ikinci Higgs bozonunun 125 GeV'deki en hafif CP-çift Higgs bozununa dejenere olacağı ve Higgs'in iki foton bozunum kanalına katkı sağladığı gösterilmiştir. Buna ek olarak, dejenere olmasa da yine aynı Higgs bozonu  $\sim 145$  GeV kütle skalasında  $h \rightarrow 4l$  bozunma kanalına olası bir açıklama getirmektedir.

# TABLE OF CONTENTS

LIST OF FIGURES .....	viii
LIST OF TABLES .....	x
CHAPTER 1. INTRODUCTION .....	1
CHAPTER 2. STANDARD MODEL .....	4
2.1. Main Blocks of the Standard Model.....	4
2.1.1. Spontaneous Symmetry Breaking .....	5
2.1.2. Decay and Production Channels of Higgs .....	10
2.2. Problems of SM .....	12
2.2.1. Gauge Hierarchy Problem .....	14
CHAPTER 3. BASICS OF SUPERSYMMETRY AND MINIMAL SUPERSYMMETRIC STANDARD MODEL(MSSM) .....	17
3.1. Supersymmetry Algebra .....	17
3.1.1. The Lagrangian for Non-Interacting Wess-Zumino Model .....	19
3.1.2. Introducing F terms and D terms .....	20
3.1.3. Superpotential .....	22
3.1.4. SUSY Breaking .....	24
3.2. MSSM .....	25
3.2.1. R-parity .....	26
3.3. Successes and Problems of the MSSM.....	27
3.3.1. Higgs Boson Excesses in CMS .....	29
CHAPTER 4. B-L SYMMETRIC SSM .....	31
4.1. $U(1)_{B-L}$ Extension of MSSM .....	31
4.1.1. Model Description .....	32
4.1.2. Soft SUSY Breaking in BLSSM .....	34
4.1.3. The Higgs Sector of BLSSM .....	35
4.1.4. The Right-Handed Neutrino Contribution .....	37

CHAPTER 5. MASS SPECTRUM AND HIGGS BOSON DECAYS IN BLSSM ..	39
5.1. Scanning Procedure and the Experimental Constraints .....	39
5.2. Mass Spectrum .....	41
5.3. Higgs Boson Decays .....	46
5.3.1. $h \rightarrow \gamma\gamma$ .....	46
5.3.2. $h \rightarrow 4l$ .....	49
CHAPTER 6. CONCLUSION .....	51
REFERENCES .....	52

# LIST OF FIGURES

<u>Figure</u>	<u>Page</u>
Figure 2.1. Higgs potential before (left) and after (right) spontaneously symmetry breaking .....	7
Figure 2.2. Production Channels of Higgs Boson in the SM .....	10
Figure 2.3. Decay Channels of Higgs Boson in the SM .....	11
Figure 2.4. Higgs boson decay to two photon via top quark or W boson loop .....	12
Figure 2.5. Quantum corrections to higgs masses after interacting with fermions, itself and gauge bosons respectively .....	15
Figure 2.6. Supersymmetry (SUSY) defines a superpartner to each particle to cancel quadratic quantum corrections .....	16
Figure 3.1. Proton decays via R-parity violating $\tilde{s}_R^*$ interaction .....	27
Figure 3.2. Evaluation of gauge couplings in SM (left) and MSSM (right) .....	28
Figure 3.3. CMS data for Higgs boson decays to two photons and Higgs boson decays to four leptons .....	29
Figure 3.4. Mass of the second lightest Higgs boson vs mass of the SM-like Higgs boson in MSSM .....	30
Figure 4.1. The effective Yukawa interactions between the singlet Higgs boson and fermions. The top diagrams illustrate the non-SUSY loops, while the bottom diagrams displays the SUSY interference. ....	36
Figure 5.1. Plots in $m_0 - M_{1/2}$ , $m_0 - A_0/m_0$ , $m_0 - \tan \beta$ , and $g_{YB}(\text{GUT}) - g_{YB}(\text{SUSY})$ planes. All points are consistent with REWSB. Green points satisfy the mass bounds and the constraints from the rare B-decays. Blue points form a subset of green, and they represent solutions with $m_{h_2} \leq 150$ GeV. ....	41
Figure 5.2. Plots in the $M_{\text{SUSY}} - v_X$ , $m_{N_2} - m_{N_1}$ , $M_{\tilde{N}_1} - v_X$ , and $m_{\tilde{N}_2} - m_{\tilde{N}_1}$ planes. The color coding is the same as Figure 5.1. The solid line in the $M_{\text{SUSY}} - v_X$ plane indicates the regions where $M_{\text{SUSY}} = v_X$ . ....	42
Figure 5.3. Plots in $m_{\tilde{t}_1} - m_{\tilde{\chi}_1^0}$ , $m_{\tilde{b}_1} - m_{\tilde{\chi}_1^0}$ , $m_{\tilde{\tau}_1} - m_{\tilde{\chi}_1^0}$ , and $m_{\tilde{\chi}_1^\pm} - m_{\tilde{\chi}_1^0}$ planes. The color coding is the same as Figure 5.1. In addition, the solid line shows the degenerate mass region in each plane. ....	43
Figure 5.4. Plots in $m_{\tilde{q}} - m_{\tilde{g}}$ and $m_{\tilde{\mu}_L} - m_{\tilde{\mu}_R}$ planes. The color coding is the same as Figure 5.1. ....	44



- Figure 5.5. Plots in  $m_{h_2} - m_{h_1}$  and  $m_{h_3} - m_{A_1}$  planes. The color coding is the same as Figure 5.1 except that the Higgs mass bound in green is not applied in the  $m_{h_2} - m_{h_1}$  plane since  $m_{h_1}$  is plotted in one axis. The diagonal line represents the mass degeneracy. .... 45
- Figure 5.6. Plots for the Higgs boson production cross-section through GGF (top panel) and VBF (bottom panel) in the  $\sigma(gg \rightarrow h_1) - m_{h_1}$ ,  $\sigma(VB \rightarrow h_1) - m_{h_1}$ ,  $\sigma(gg \rightarrow h_2) - m_{h_2}$  and  $\sigma(VB \rightarrow h_2) - m_{h_2}$  planes. The color coding is the same as Figure 5.1, except we do not apply the SM Higgs boson constraint ( $m_{h_1} \sim 125$  GeV) to the left panel, since  $m_{h_1}$  is directly plotted here. Similarly, the condition  $m_{h_2} \leq 150$  GeV, represented by the blue region, is not applied to the right panels, since  $m_{h_2}$  is on the horizontal axis. .... 47
- Figure 5.7. Plots in  $R_{\gamma\gamma}^1 - m_{h_1}$ ,  $R_{\gamma\gamma}^2 - m_{h_2}$  and  $R_{\gamma\gamma}^{\text{eff}} - m_h^{\text{eff}}$  planes. The color coding is the same as Figure 5.6. The red dashed line indicates the observed cross-section in  $h \rightarrow \gamma\gamma$  normalized to the SM prediction. .... 48
- Figure 5.8. Plots in  $R_{ZZ}^1 - m_{h_1}$  and  $R_{ZZ}^2 - m_{h_2}$ . The color coding is the same as Figure 5.6. The dashed line indicates the observed cross-section, while the solid line represents the expected cross-section without the Higgs boson. .... 49

# LIST OF TABLES

<u>Table</u>		<u>Page</u>
Table 3.1.	Number of bosonic and fermionic degrees of freedom in Chiral Lagrangian .....	20
Table 3.2.	Number of bosonic and fermionic degrees of freedom in Gauge Lagrangian .....	22
Table 4.1.	Chiral (Matter) Supermultiplets in the BLSSM .....	32
Table 4.2.	Gauge (Vector) Supermultiplets in the BLSSM .....	32

# CHAPTER 1

## INTRODUCTION

One of the most essential property of human being is the aspiration which leads people to explain the natural phenomena. The questions of “What is the building block of nature?” and “What are the fundamental structures and how do they interact with each other?” always make scientists excited in every period of history. As an answer to these questions the Standard Model (SM) constructed by Weinberg, Salam and Glashow in 1964 opened a new era in understanding of the elementary particles and explanation of three of four fundamental interactions of nature the so-called electromagnetic, weak and strong interactions. According to the SM, elementary particles are divided into two groups as fermions and bosons. Elementary particles which constitute the matter are called fermions. Fermions are particles having fractional spin and obey to the Fermi-Dirac statistics. Fermion group include the quarks and leptons. In addition to this, the SM also explains how the basic building blocks of matter interact. These interactions are mediated by spin-1 particles which are called gauge bosons. These spin-1 particles which are responsible for carrying physical forces are called bosons and obey the Bose-Einstein statistics. The mediators of the strong, weak and electromagnetic interactions are, respectively, gluon,  $W^\pm$ ,  $Z^0$  bosons and photon. Each type of interactions corresponds the gauge symmetry group and the theory exhibits an exact invariance under the combination of these symmetries. Therefore, the SM basically depends on a certain gauge principle according to which all the forces of nature are mediated by the exchange of the gauge fields of the corresponding local gauge symmetry group.

In the SM, this gauge symmetry forbids mass terms for fermions and gauge bosons. That is why we need to break the symmetry and allow particles to have their masses. Hence, the origin of both gauge boson and fermion masses is explained with the help of the electroweak symmetry breaking (EWSB). This spontaneous symmetry breaking is implemented by means of the Higgs mechanism. In the Higgs mechanism [2], a scalar Higgs field develops a non-zero vacuum expectation value (VEV) through its potential, which includes also self-interactions of the Higgs fields, and the particles acquire their masses proportionally to this VEV and their Yukawa couplings to the Higgs field. In addition, the three Goldstone bosons, which emerge within the spontaneous breaking of the electroweak symmetry breaking, are swallowed by  $W^\pm$  and  $Z^0$  bosons such that these

gauge bosons become massive. At the end, one scalar boson remains after EWSB, which is called the Higgs boson. With the discovery of the Higgs boson of mass about 125 - 126 GeV by the ATLAS [3] and the CMS [4] experiments, analyses have confirmed that the SM predictions are in a very good agreement with the observations. Hence, this discovery provided extra motivation for future studies on new physics beyond the SM. In Chapter 2, we will examine the properties of Higgs particle boson and we will point out the serious problem about the radiative corrections to the Higgs boson mass in detail.

Although the SM has been completed with the Higgs boson discovery and confirmed in numerous high energy experiments with great precision in the past decades, there is no doubt that the SM is not a fundamental theory, since it cannot provide any explanation concerning the gauge hierarchy problem between the electroweak scale and the Planck Scale ( $M_{Pl}$ ) [9], the absolute stability of the Higgs potential [10], neutrino oscillations, dark matter, baryon asymmetry in the universe, family problem, the unification of fundamental forces etc. Because of unanswered questions in the SM based on gauge hierarchy problem, neutrino oscillations, we need a covering model beyond the SM that is broken into the SM at low scales. In Chapter 2, we will examine the properties of the Higgs boson. We will give a brief introduction about the unanswered problems and we concentrate on the hierarchy problem which is the main motivation of the new physics beyond the SM. Then, we will introduce an elegant solution as a further symmetry for stabilizing dangerously large radiative corrections to Higgs boson mass. This new symmetry which is firstly proposed to solve gauge hierarchy problem by J. Wess and B. Zumino in 1974 is called as supersymmetry (SUSY) whose basic concepts will be discussed in detail in Chapter 3.

SUSY is simply a symmetry that relates the fermion and bosons to each other with supersymmetric transformations. Interestingly, If two successive SUSY transformations are applied to a particle, the spin remains the same, but the field is shifted in space-time. In this context, SUSY is the only known symmetry that relates the internal symmetries with the space-time symmetries. The Minimal Supersymmetric Standard Model (MSSM) which is the first realistic supersymmetric version of the SM was proposed in 1981 by Howard Georgi and Savas Dimopoulos, is the minimal supersymmetric extension of the SM. Besides this, we give a discussion about the MSSM in regard to its symmetries, gauge structure as well as particle and superpartner spectrum in Chapter 3. For example, the Higgs sector of the MSSM can be summarized as following. There are two Higgs doublets in the MSSM contrary to the SM. While in the SM there is only one Higgs boson, in the MSSM five Higgs bosons arise: two of them are neutral and CP even scalar

Higgs bosons ( $h$  and  $H$ ), two of them are charged Higgs bosons ( $H^\pm$ ) and the rest is the neutral and CP odd pseudoscalar Higgs boson ( $A$ ).

Even though MSSM can provide possible explanations to some of the problems, particularly to the gauge hierarchy problem, it leaves others unanswered. We emphasize excesses in certain Higgs boson decay channels in  $h \rightarrow \gamma\gamma$  [12] and  $h \rightarrow ZZ \rightarrow l^+l^-l^+l^-$  channels [13]. Even though MSSM has five physical Higgs states, we conclude that such excesses cannot be explained within the MSSM Higgs bosons if one considers SUSY GUT models in which an underlying GUT gauge group breaks into the MSSM at the GUT scale. We proposed that these excesses can be explained if one considers an extra  $U(1)_{B-L}$  which is spontaneously broken at some scale of order TeV. In Chapter 4, we study characteristic properties of supersymmetric  $U(1)_{B-L}$  model, and explain the differences from the MSSM.

Finally, in Chapter 5, we discuss our scanning method and the experimental constraints that we apply to deal with the experimental observations. After we present mass spectrum of some particles, especially those pertaining to decay channels that we would like to explain, we emphasize the Higgs boson decays in supersymmetric  $U(1)_{B-L}$  model. We show that the observed excesses in the Higgs sector can be accommodated in SUSY B-L model and conclude the thesis with the discussion of the result of our analysis. This study is published with the title “Mass Spectrum and Higgs Profile in BLSSM” in Phys. Rev. D 93, 055024.

## CHAPTER 2

### STANDARD MODEL

As a main success of 20th century particle physics, the questions of how the fundamental particles interact and how three of four forces are related to each other are included in an elegant way in the Standard Model of particle physics.

#### 2.1. Main Blocks of the Standard Model

In this section, we will describe the SM without giving all the details. Detailed reviews and books can be found in the literature [5–8]. The SM is a theory that explains the particles that have been discovered so far and three of four fundamental forces which are important for interactions of these particles. These three forces are electromagnetic, strong and weak forces. One of the biggest success of the SM is to calculate the properties of the particles and the interactions between them with great precision. The SM is briefly a gauge theory of spin 0, 1/2 and 1 particles based on  $SU(3)_C \times SU(2)_L \times U(1)_Y$  gauge symmetry group with subscripts C, L, Y that refer to color, left chirality and weak hypercharge.  $SU(2)_L \times U(1)_Y$  governs the electroweak interactions and  $SU(3)_C$  describes the strong interactions. For each gauge group there are corresponding generators and each generator constitutes a “vector field”. These vector fields keep lagrangian invariant by gauging itself under the local transformations. Therefore, these vector fields which are carriers of physical forces are also called as “gauge fields”.

In the SM, particles are organized in two groups as fermions and bosons. Fermions are particles having half spin. They obey Fermi-Dirac Statistics. In the SM, the fermions are divided into three families. These three families are identical to each other, except their masses. The ordinary matter is constituted by the first families, while the heavier families are rather unstable and decay to the particles of the first families. Leptons are organized as singlets under  $SU(3)_C$ . In other words, they do not carry color charge; and hence, they do not participate in the strong interactions. They join only to the electroweak interactions. However, quarks are color triplets. Namely, each quark flavour carries three colors. Since quarks have both color charge and hyper-charges, they participate both strong and electroweak interactions. According to solution of Dirac equation, we have left

with left and right handed particles. Left handed particles are defined as doublets under  $SU(2)_L \times U(1)_Y$  symmetry by giving them the same hypercharge, while the right-handed particles are singlets under  $SU(2)_L$ . In this context,  $SU(2)_L$  forms a chiral theory, since it distinguishes the left-handed particles from the right-handed ones. On the other hand, bosons are particles having integer spin. They obey Bose-Einstein Statistics and they are force carrier particles.  $SU(3)_C$  has 8 generators (with  $3^2 - 1 = 8$  generators) which are 8 gluons ( $G_\mu^a, a=1,2,\dots,8$ ) of  $SU(3)_C$ . 3 generators of  $SU(2)_L$  ( $W_\mu^a, a=1,2,3$  gauge fields) and 1 generator of  $U(1)_Y$  ( $B_\mu$  gauge field) associate with  $W_\pm, Z_0$  which are mediator of the weak interactions and the photon as the mediator of the electromagnetic interactions.

$$SU(3)_C \longrightarrow 8 \text{ gauge boson (Gluons } G_\mu^a)$$

$$SU(2)_L \longrightarrow 3 \text{ gauge boson (} W_\pm, Z_0)$$

$$U(1)_Y \longrightarrow 1 \text{ gauge boson (} B_\mu)$$

These 12 gauge bosons are massless at high energies, however at low energies  $SU(2)_L \times U(1)_Y$  symmetry breaks down to  $U(1)_{EM}$  through the spontaneous symmetry breaking, with which the gauge bosons acquire their masses. The mechanism behind this symmetry breaking is called the Higgs Mechanism. Therefore, in order to be consistent masses for all fermions and vector bosons, SM predicts a scalar (spin=0) Higgs boson which is experimentally observed in CERN in 2012, July.

### 2.1.1. Spontaneous Symmetry Breaking

The electroweak part of the SM distinguishes the left-handed and right-handed fermions and hence it forms a chiral theory. The subscript ‘‘L’’ in  $SU(2)_L$  refer that  $SU(2)_L$  acts only on left-handed fermions and is blind to right-handed ones. Therefore, in the formalization of the SM, left-handed fermions reside in  $SU(2)_L$  doublets, while right-handed ones are singlet. In the electroweak Lagrangian, it could be easily seen that left-handed and right-handed particles transform differently under  $SU(2)_L \times U(1)_Y$ .

$$\mathcal{L}_{EW} = \bar{\Psi}_R \gamma^\mu D_\mu^{(R)} \Psi_R + \bar{\Psi}_L \gamma^\mu D_\mu^{(L)} \Psi_L \quad (2.1)$$

where

$$D_\mu^{(L)} = \partial_\mu - \frac{ig_L}{2} W_\mu^i \cdot \sigma^i - \frac{ig_Y}{2} B_\mu$$

$$D_\mu^{(R)} = \partial_\mu - \frac{ig_Y}{2} B_\mu$$

Left-handed particles transform as  $\Psi_L \rightarrow \Psi'_L = \exp(-\frac{ig_L}{2} W_\mu^i \cdot \sigma^i) \Psi_L$  under  $SU(2)_L$  transformations, whereas right-handed particles remain unchanged (i.e.  $\Psi_R \rightarrow \Psi'_R = \Psi_R$ ). This arises from the fact that right-handed fermions do not have  $SU(2)_L$  charge.

When one writes down the electroweak Lagrangian, one can also think to write a mass term,  $m\psi\bar{\psi} = m(\bar{\psi}_R\psi_L + \bar{\psi}_L\psi_R)$ , for fermion fields at first sight. Since if the unit analysis is processed, it seems like there is no obstruction to write down such a term. However, mass term of fermions contains mixing of the left and right handed fermions and since left-handed and right-handed fermions transform differently under  $SU(2)_L \times U(1)_Y$ , one can easily see that the Lagrangian is not invariant with such a mass term. Therefore, mass terms of fermions are forbidden by  $SU(2)_L \times U(1)_Y$  symmetry in the electroweak Lagrangian.

$$\mathcal{L}_{EW} = \bar{\Psi}_R \gamma^\mu D_\mu^{(R)} \Psi_R + \bar{\Psi}_L \gamma^\mu D_\mu^{(L)} \Psi_L + \cancel{m(\bar{\Psi}_R \Psi_L + \bar{\Psi}_L \Psi_R)} \quad (2.2)$$

However, experiments show that the fermions are massive. To obtain mass terms of fermion, a new complex scalar doublet Higgs field,  $\Phi = \begin{pmatrix} \phi_1 \\ \phi_2 \end{pmatrix}$  is introduced as an  $SU(2)_L$  doublet with no color charge. This Higgs complex scalar field interacts with fermions as indicated below in the Yukawa Lagrangian which is written for only first families.

$$\mathcal{L}_y = y_d \bar{Q} \Phi d_R + y_R \bar{L} \Phi e_R + y_u \bar{Q} \Phi^c u_R + \dots \quad (2.3)$$

where  $Q = \begin{pmatrix} u_L \\ d_L \end{pmatrix}$  and  $L = \begin{pmatrix} \nu_{eL} \\ e_L \end{pmatrix}$

To be able to conserve hypercharge in the electroweak interactions, total hypercharge of each term in the Yukawa Lagrangian must be zero. This is satisfied if hypercharge of our complex scalar Higgs field is 1. Then it turns out that according to the Gell-Mann-Nishijima formula, the upper component of the complex Higgs doublet has electric charge 1, whereas the lower component is neutral as indicated below where  $\tau_3$  stands for the isospin.



$$\Phi = \begin{pmatrix} \phi_1 \\ \phi_2 \end{pmatrix} \begin{array}{l} \longrightarrow \tau_3 = 1/2, Y = 1, \text{ then } Q_{EM} = +1 \\ \longrightarrow \tau_3 = -1/2, Y = 1, \text{ then } Q_{EM} = 0 \end{array} \longrightarrow \Phi = \begin{pmatrix} \phi^+ \\ \phi^0 \end{pmatrix}$$

Another important point in the Yukawa Lagrangian is that d-type quarks masses are generated with the interaction of the Higgs field itself, while the masses of the u-type quarks are obtained with the interaction of the charge conjugation of the Higgs scalar field. The Higgs field has a non-zero VEV, which induces the mass terms for the fermions. Higgs potential is introduced in Eq. 2.4 where  $\lambda$  is always defined as positive to satisfy vacuum stability. If we have a higgs potential in the form below, two different configuration is possible according to sign of  $\mu^2$  as represented in Fig. 2.1.

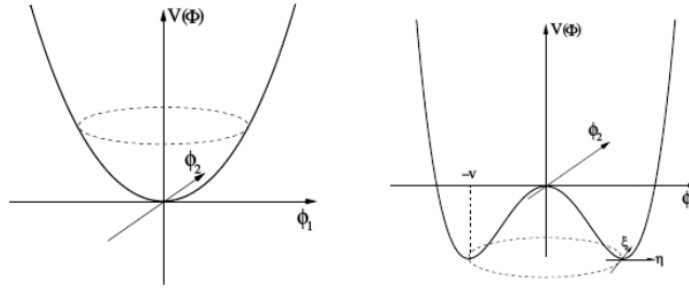


Figure 2.1. Higgs potential before (left) and after (right) spontaneously symmetry breaking

For the positive value of  $\mu^2$ , it gives zero vacuum expectation value, whereas for the negative value of  $\mu^2$ , it gives non-zero vacuum expectation value.

$$V(\phi) = \frac{1}{2}\mu^2\phi^2 + \frac{1}{4}\lambda\phi^4 \quad (2.4)$$

$$\frac{\partial V(\phi)}{\partial \phi} = \phi(\mu^2 + \lambda\phi^2) = 0$$

$$\mu^2 > 0 \longrightarrow v = \langle \phi \rangle = 0$$

$$\mu^2 < 0 \longrightarrow v = \langle \phi \rangle = \pm \sqrt{\frac{-\mu^2}{\lambda}} \quad (2.5)$$

When the Higgs scalar field develops its VEV due to its desire to be at the minimum potential energy, the fermion mass terms, which could not be written in electroweak

lagrangian, are obtained by spontaneously symmetry breaking. The fact that gauge bosons of weak interactions ( $W_{\pm}$ , Z bosons) are massive and photon as a mediator of electromagnetic interactions is massless alludes to  $SU(2)_L \times U(1)_Y$  symmetry breaking to  $U(1)_{EM}$  symmetry. Note that the Higgs field does not carry any color charge; and hence, its non-zero VEV does not break the  $SU(3)_C$  symmetry. In this sense, the gluons remain massless after the electroweak symmetry breaking, but  $SU(3)_C$  forms a confined symmetry.

Since Higgs field is described as a doublet and complex scalar, it has four degree of freedom. After the spontaneous symmetry breaking, three massless Higgs bosons arise in addition to one massive Higgs boson. These massless Higgs bosons which are called ‘‘Goldstone Bosons’’ are swallowed by  $W_{\pm}$  and Z bosons and the remaining massive one arises as the physical state called the Higgs boson.

As fermions acquire their masses via Yukawa interactions, the masses of gauge bosons are gained through the gauge interactions. To give a mass to gauge bosons, one has to handle with kinetic terms associated with the Higgs field in the Lagrangian indicated as follow.

$$\mathcal{L}_{kin} = \frac{1}{2}(D_{\mu}\Phi)^{\dagger}(D^{\mu}\Phi) \quad (2.6)$$

where  $\Phi$  is given as follows after it develops VEV.

$$\Phi = \begin{pmatrix} 0 \\ v + h \end{pmatrix} \quad (2.7)$$

While  $v$  denotes the VEV of the neutral Higgs field,  $h$  represents the perturbative effects around the vacuum expectation value. Since  $\phi_1$  is charged Higgs field, its VEV must be zero not to violate the charge conservation.  $D_{\mu}$  in the Equation 2.6 is defined as follows under  $SU(2)_L \times U(1)$  symmetry.

$$D_{\mu} = \partial_{\mu} - \frac{ig_L}{2}W_{\mu}^i \cdot \sigma^i - \frac{ig_Y}{2}B_{\mu} \quad (2.8)$$

After expanding  $(D_{\mu}\Phi)^{\dagger}(D^{\mu}\Phi)$  expression, one comes up with the terms which is arranged in  $v^2$ ,  $hv$  and  $hh$  parantheses as represented in Equation 2.9.

$$(D_{\mu}\Phi)^{\dagger}(D^{\mu}\Phi) = v^2 \left( \frac{g_L^2}{2}W_{\mu}^{-}W^{\mu+} + \frac{g_L^2}{8}W_{\mu}^3W^{\mu3} - \frac{g_L g_Y}{4}W_{\mu}^3B^{\mu} + \frac{g_Y^2}{8}B_{\mu}B^{\mu} \right)$$

$$\begin{aligned}
& +hv \left( \frac{g_L^2}{\sqrt{2}} W_\mu^- W^{\mu+} + \frac{g_L^2}{2\sqrt{2}} W_\mu^3 W^{\mu3} - \frac{gLg_Y}{\sqrt{2}} W_\mu^3 B^\mu + \frac{g_Y^2}{2\sqrt{2}} B_\mu B^\mu \right) \\
& +hh \left( \frac{g_L^2}{2} W_\mu^- W^{\mu+} + \frac{g_L^2}{4} W_\mu^3 W^{\mu3} - \frac{gLg_Y}{2} W_\mu^3 B^\mu + \frac{g_Y^2}{4} B_\mu B^\mu \right) \quad (2.9)
\end{aligned}$$

where  $W_\mu^+$  and  $W_\mu^-$  are defined as follows, respectively.

$$W_\mu^+ = \frac{1}{\sqrt{2}} (W_1 - iW_2) \quad W_\mu^- = \frac{1}{\sqrt{2}} (W_1 + iW_2) \quad (2.10)$$

It turns out that the terms in the  $v^2$  paranthesis in Equation 2.9 are the mass terms of weak gauge bosons. These bosons acquire their masses with respect to magnitude of the coupling constant  $g$ . The first term stands for the mass term of  $W^-$  and  $W^+$  bosons. Nevertheless, the mass of  $Z^0$  boson cannot be obtained from the second, third and the fourth terms since the mass of  $Z^0$  boson exists in a mixture of  $W_\mu^3$  and  $B_\mu$  fields. Therefore, the mass of  $Z$  boson can be extracted after diagonalising the second, third and the fourth terms.

$$\frac{1}{8} \begin{pmatrix} W_\mu^3 & B_\mu \end{pmatrix} \begin{pmatrix} g_L^2 & -gLg_Y \\ gLg_Y & g_Y^2 \end{pmatrix} \begin{pmatrix} W_\mu^3 \\ B_\mu \end{pmatrix} = \begin{pmatrix} A_\mu & Z_\mu \end{pmatrix} \begin{pmatrix} a & 0 \\ 0 & b \end{pmatrix} \begin{pmatrix} A_\mu \\ Z_\mu \end{pmatrix} \quad (2.11)$$

Then,  $A_\mu, Z_\mu, W_\mu$  and  $B_\mu$  can be obtained as follows.

$$\begin{aligned}
W_\mu^3 &= \cos(\theta)A_\mu - \sin(\theta)Z_\mu & B_\mu &= -\sin(\theta)A_\mu + \cos(\theta)Z_\mu \\
Z_\mu &= -\sin(\theta)W_\mu^3 + \cos(\theta)B_\mu & A_\mu &= \cos(\theta)W_\mu^3 + \sin(\theta)B_\mu \quad (2.12)
\end{aligned}$$

where  $\theta$  is called ‘‘Weinberg angle’’ and responsible for the mixing. It is represented in the following way.

$$\sin(\theta) = \frac{g_Y}{\sqrt{g_Y^2 + g_L^2}} \quad \cos(\theta) = \frac{g_L}{\sqrt{g_Y^2 + g_L^2}} \quad (2.13)$$

Then, one can obtain the following expression which the mass terms of  $W^+, W^-$  and  $Z^0$  bosons can be seen easily.

$$(D_\mu \Phi)^\dagger (D^\mu \Phi) = \frac{1}{8} v^2 \left[ \left( \frac{g_L^2}{2} W_\mu^- W^{\mu+} \right) + (g_L^2 + g_Y^2) Z_\mu Z^\mu \right] + \dots \quad (2.14)$$

In Eq. 2.14, the mass of  $W^-$  and  $W^+$  bosons are dependent only on the constant  $g_L$  whereas the mass of  $Z^0$  boson depends on both the constant  $g_L$  and  $g_Y$ . After diagonalisation process, variable “a” in Eq. 2.11 is obtained to be equal to zero which refers to the massless photon.

## 2.1.2. Decay and Production Channels of Higgs

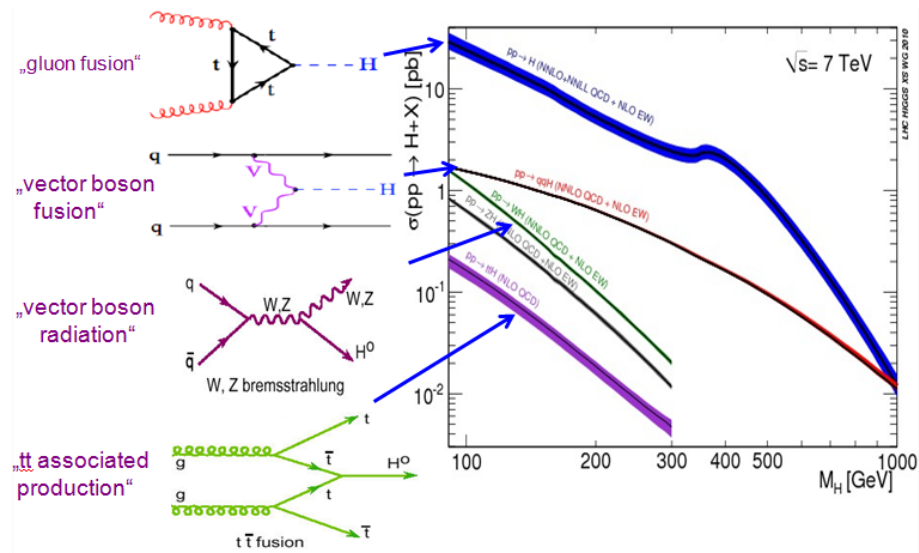


Figure 2.2. Production Channels of Higgs Boson in the SM

When one calculates the  $(D_\mu \Phi)^\dagger D^\mu \Phi$  expression as indicated in Eq. 2.9, one also comes up with the terms which can be seen in the  $vh$  and  $hh$  parentheses in addition to the mass terms of weak gauge bosons in the  $v^2$  parentheses. The terms in the  $vh$  parentheses show production and decay channels of single higgs boson at tree level whereas the terms in the  $hh$  parenthesis represent production and decay channels of two higgs bosons at tree level. However, the biggest cross section in the Higgs boson production comes from gluon-gluon fusion (GGF) in the SM as represented in Fig. 2.2 even though Higgs

boson does not have a tree level coupling with gluon directly. In GGF the Higgs boson is produced through a loop level process in which the quarks run in the loop. Even though all quarks can, in principle, contribute to the Higgs boson production process, top and bottom quarks give the biggest contributions because of their large Yukawa couplings to the Higgs boson. The second biggest contribution comes from vector boson fusion. Each of two quarks can radiate a vector boson as can be seen from Fig. 2.2 and since Higgs boson has a coupling with  $W_\mu^- W^{\mu+}$  and  $Z_\mu Z^\mu$  at tree level, these two produced vector bosons interact with the Higgs boson. Therefore, Higgs boson can also be produced in this way. In addition to these production channels, Higgs boson can also be produced through vector boson radiation and  $t\bar{t}$  associated production. However, contributions coming from these production channels are generally negligible in comparison to the gluon-gluon fusion and vector boson fusion. We will again refer gluon-gluon fusion and vector boson fusion in subsection 5.3.1 when we discuss Higgs boson production in the framework of supersymmetric B-L model.

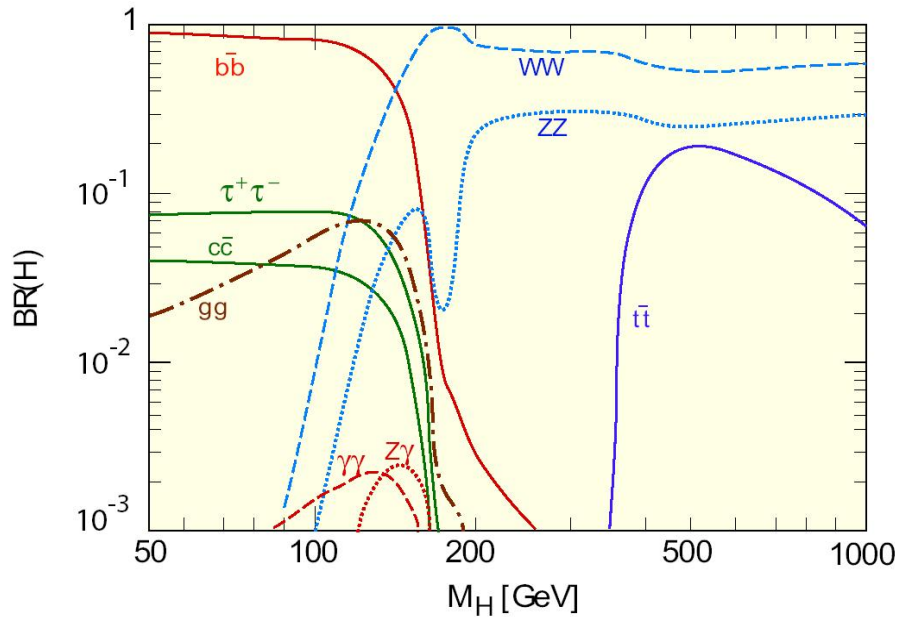


Figure 2.3. Decay Channels of Higgs Boson in the SM

When Higgs boson decay channels are examined, Higgs to  $b\bar{b}$  decay channel dominates the region below 150 GeV as demonstrated in Fig. 2.3. In this region, Higgs boson mass is not sufficient to decay to two W bosons or two Z bosons. However, above 150 GeV, Higgs to  $W^+W^-$  and  $Z^0Z^0$  are the most important decay channels since mass of Higgs is sufficient to decay into two W bosons or two Z bosons. Even though Higgs boson

does not have a coupling with  $\gamma\gamma$  and  $Z\gamma$  at tree level, Higgs boson can decay into  $\gamma\gamma$  or  $Z\gamma$  through loop level as represented in Fig. 2.4.

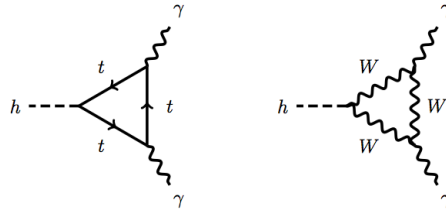


Figure 2.4. Higgs boson decay to two photon via top quark or W boson loop

## 2.2. Problems of SM

Even though the Standard Model (SM) is consistent with the experimental results in almost all its predictions, it is still far from being a complete theory due to the lots of unexplained arbitrary parameters and unexplained problems. Some of the problems which SM suffers are summarized as follows:

**Gauge Hierarchy Problem** : In the SM, a doublet Higgs field is introduced to generate masses for weak gauge bosons and fermions. When the Higgs boson mass is calculated at tree level, its mass is obtained around electroweak scale. Besides that, the Higgs boson mass must remain stable in a theoretical consistent model. However, quantum corrections from every particle that couples directly or indirectly to the Higgs field yield enormous contributions to Higgs boson mass. This is known as “Gauge Hierarchy Problem”. This problem will be analysed in more detail in subsection 2.2.1.

**Neutrino Masses and Mixings** : According to the minimal version of the SM, the right-handed neutrino is not included in the theory. Therefore, left-handed neutrinos cannot acquire their masses even after the electroweak symmetry breaking since mass term contains both left and right-handed spinors and right-handed neutrinos have not been observed experimentally yet. On the other hand, although neutrino masses are predicted much lighter compared to the other fermions, the experimental measurements support that the neutrinos must have mass.

**Baryon Asymmetry Problem** : The SM does not explain the dominance of matter with respect to anti-matter. There are convincing clues that the amounts of matter and

anti-matter were equal at high energies as the solution of Dirac equation described. However, as the temperature decreases after Big Bang, this symmetry is somehow broken. As a consequence of this, we live in a matter dominated universe. The source of this asymmetry can be characterized with the CP violation which is firstly observed in neutral Kaon meson. However, the amount of CP violation in the SM is not sufficient to generate the observed baryon asymmetry in the universe.

**Dark Matter** : Based on the cosmological observations, the standard model is able to explain only about 4% of the universe. This observation states that 23% of the energy density of the universe should be formed by dark matter which does not interact via electromagnetic interactions. In the SM, there is no suitable candidate particle for dark matter which is proposed as durable and only interacting weakly with standard model particles.

**Family Problem** : All observed matter is generated by only the first family ( $\nu_e$ ,  $e^-$ , u, d). However, existence of two more families ( $\nu_\mu$ ,  $\mu^-$ , c, s) and ( $\nu_\tau$ ,  $\tau^-$ , t, b) has been proved by experiments. Second and third families are just heavier copies of the first family and they eventually decay to the first family particles and do not participate in forming the existent matter. Hence, the SM cannot give an appropriate explanation to the question of why second and third families of quarks and leptons exist in the universe.

**Fermion Masses** : It seems that Higgs mechanism can explain the fermion masses precisely. However, the value of the fermion masses is related to the Yukawa coupling which described the strength of the interaction of Higgs boson and fermions. Yet this coupling cannot be determined in the SM and are expressed as a free parameter in the theory.

**Gauge Symmetry Problem** : The SM has a direct product of three groups  $SU(3)_C \times SU(2)_L \times U(1)_Y$  with their different corresponding arbitrary gauge couplings. However, SM does not provide deep explanation to understand the origin of these different gauge groups. In addition, there is no understanding for the parity violating chiral feature of electroweak part of SM. Moreover, since SU(2) charge and hypercharge of fermions under its gauge group are assigned to obtain the correct electric charge of each fermion, they are completely arbitrary quantum numbers.

**Electrical Charge Quantization** : The Standard Model has no explanation to the question of why electric charges of particles are always quantized with the multiples of  $e/3$  to form neutral atoms and stabilize the matter.

**Gauge Coupling Unification** : According to the Standard Model, gauge couplings corresponding to three fundamental forces do not unified at any energy scale.

However, in Grand Unified Theories (GUT), only one single symmetry group and its corresponding gauge coupling is proposed at high energies. Since the SM is approved at the low scales, this single gauge group should consist of the SM as a subgroup, and its breaking mechanism can enlighten the origin of the SM gauge groups. On the other hand, the gauge couplings unify at Grand Unification Scale ( $M_{GUT} \approx 10^{16}$  GeV) and it provides a strong motivation for SUSY GUTs.

### 2.2.1. Gauge Hierarchy Problem

As summarized briefly above, one of the most important problems of the SM is known as the ‘‘Gauge Hierarchy Problem’’. Gauge hierarchy problem arises from the contributions to the Higgs boson mass resulting from quantum corrections when we take the loop level interactions into account. Every particle that interacts with the Higgs field generates tremendous contributions to its mass. If there is no other accepted theory between the Plank scale and electroweak scale, Planck scale can be accepted as the cut-off scale ( $\Lambda_{UV}$ ). In this way, radiative corrections to the Higgs boson mass squared have scale of  $10^{38}$  GeV<sup>2</sup>. This quantum corrections depend on Yukawa couplings, self interaction coupling of Higgs boson and gauge boson couplings as represented in Fig. 2.5.

These contributions diverge quadratically in terms of the cut-off scale as indicated in Eq. 2.15, 2.16 and 2.17.

$$\delta_f m_H^2 \approx -\frac{|\lambda_f|^2}{16\pi^2} \Lambda_{UV}^2 \quad (2.15)$$

$$\delta_H m_H^2 \approx \frac{\lambda_s}{8\pi^2} \Lambda_{UV}^2 \quad (2.16)$$

$$\delta_g m_H^2 \approx \frac{|g|^2}{16\pi^2} \Lambda_{UV}^2 \quad (2.17)$$

Contributions to Higgs boson mass are much larger than Higgs boson’s own mass. To cancel these corrections, the amount of required fine-tuning is enormous. In the SM, quadratic divergences are present only in the Higgs sector because fermions and bosons have chiral and gauge symmetries respectively to protect their own masses and they depend on cut-off scale ( $\Lambda_{UV}$ ) as logarithmically. However, Higgs boson mass is not protected by any symmetry.

As indicated in Eq. 2.15 and 2.17, bosonic and fermionic loops yield contributions with different sign. Therefore, supersymmetry (SUSY) can cancel this contributions in



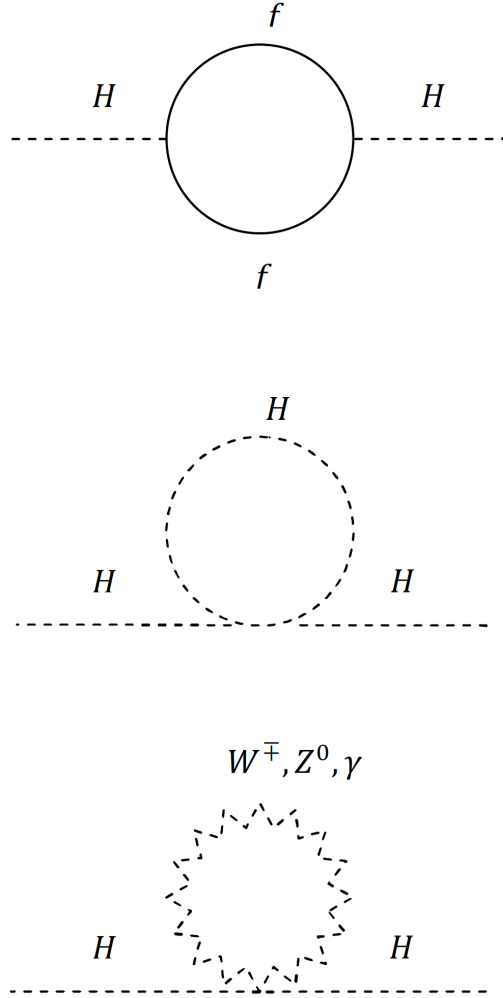


Figure 2.5. Quantum corrections to higgs masses after interacting with fermions, itself and gauge bosons respectively

a elegant way by defining a fermionic partner for each boson and vice versa as demonstrated in Fig. 2.6. In order to cancel the contribution in Eq. 2.15 resulting from the fermion loop, the coupling of the fermion loop and the coupling of the corresponding bosonic superpartner must be equal, that is,  $\lambda_f = g$ . Besides that, Higgsino loop which is fermionic superpartner of Higgs boson brings the contribution in Eq. 2.15. In order to cancel this contribution, there must be two Higgs boson in the theory ( $2|\lambda_f|^2 = \lambda_s$ ). As we will discuss in subsection 3.1.3, two Higgs doublet must exists in SUSY due to the holomorphic superpotential. Therefore, all ultraviolet divergences can be cancelled smoothly in SUSY.

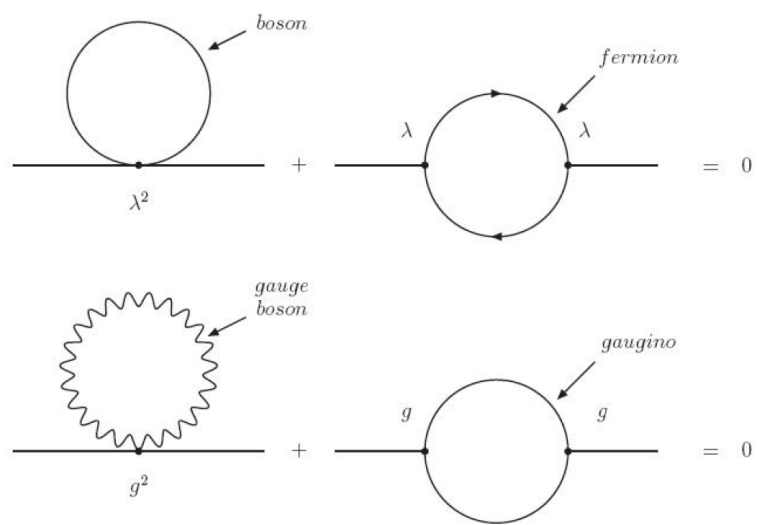


Figure 2.6. Supersymmetry (SUSY) defines a superpartner to each particle to cancel quadratic quantum corrections

## CHAPTER 3

### BASICS OF SUPERSYMMETRY AND MINIMAL SUPERSYMMETRIC STANDARD MODEL(MSSM)

The “Hierarchy Problem” of the Standard Model is the most important problem about the Higgs mass stabilization. Supersymmetry (SUSY) is one of the theories suggested to solve this problem. SUSY cancels the quadratic corrections of the Higgs mass by introducing a boson partner for each fermion and a fermion partner for each boson which are called superpartners. For this purpose, SUSY requires a transformation so-called supersymmetric transformation which turns a bosonic state into a fermionic state and vice versa. Therefore, SUSY can be simply described as a symmetry that gives a connection between fermions and bosons. SUSY generators represented by operator  $Q$  constructed in such a way that when they hit a bosonic state, they transform it to a fermionic one and vice versa.

$$\hat{Q}|Fermion\rangle = |Boson\rangle, \quad \hat{Q}|Boson\rangle = |Fermion\rangle \quad (3.1)$$

In the rest of this thesis,  $Q$  stands for the SUSY generator  $\hat{Q}$ . Since SUSY operator  $Q$  alter only spin of the particles by 1/2 unit, all quantum numbers of the particles and superpartners are exactly the same except for their spin. Interestingly, two successive SUSY transformations end with the initial state, but they shift the field in spacetime. In this context, SUSY is the only known symmetry that also relates the internal symmetries to the spacetime symmetries.

#### 3.1. Supersymmetry Algebra

In the light of success of the special relativity, any kind of relativistic model of the elementary particles should be constructed in a way that guarantees the Lorentz invariance. In this sense, the Lagrangian and relevant operators must be consistent with the relativistic transformations of the fields. In the SM, the internal symmetries and Lorentz symmetry are not really connected to each other. On the other hand, the connection between SUSY and Lorentz symmetry can be understood within the graded Lie algebra of

Poincare group in which the Poincare group generators are extended with anti-commuting operators.

The symmetry group of 4 dimensional spacetime,  $SL(2,C)$  is isomorphic to  $SU(2) \times SU(2)$  which differently transform under Lorentz transformations [5]. Hence the spinor representation of  $SL(2,C)$  should be formed by two Weyl spinors, one of which is indicated with dotted indices, while the other with the undotted ones. If one extends the Poincare algebra with the generators that transform these dotted and undotted spinors, the commutation and anti-commutation rules can be obtained as

$$\{Q_\alpha, Q_\beta\} = \{\bar{Q}_{\dot{\alpha}}, \bar{Q}_{\dot{\beta}}\} = 0 \quad (3.2)$$

$$\{Q_\alpha^i, \bar{Q}_{\dot{\beta}}^j\} = 2\delta^{ij}(\sigma^\mu)_{\alpha\dot{\beta}}P_\mu \quad (3.3)$$

$$[P_\mu, Q_\alpha^i] = [P_\mu, \bar{Q}_{\dot{\alpha}}^i] = 0 \quad (3.4)$$

$$[Q_\alpha^i, M_{\mu\nu}] = \frac{1}{2}(\sigma^{\mu\nu})_\alpha^\beta Q_\beta^i \quad (3.5)$$

$$[\bar{Q}_{\dot{\alpha}}^i, M_{\mu\nu}] = -\frac{1}{2}Q_{\dot{\beta}}^i(\bar{\sigma}^{\mu\nu})_{\dot{\alpha}}^{\dot{\beta}} \quad (3.6)$$

where  $P_\mu$  represents the generators of translations and  $M_{\mu\nu}$  stands for the generators of Lorentz transformations while the spinorial indices  $\alpha, \dot{\alpha}, \beta, \dot{\beta} = 1, 2$ , space-time indices  $\mu, \nu = 0, \dots, 3$  and  $i, j = 1, 2, \dots, N$ . If we apply the commutation rules given in Eqs.(3.5 and 3.6) for  $M_{1,2} = J_3$ , it is seen that the generators  $Q$  and  $\bar{Q}$  respectively raise and lower the spin by  $1/2$  when they hit to the particle state, and this is basically definition of the SUSY transformations.

This extended algebra which provides us a useful possibility to combine statistics of particles of integer and half-integer spin by enlarging space-time symmetries is called ‘‘Super-Poincare Algebra’’. In this thesis, we consider only unextended  $N=1$  supersymmetry which corresponds one spinor charge  $Q_\alpha$  and its conjugate  $\bar{Q}_{\dot{\alpha}}$  in order to deal with minimal particle content and due to the renormalizability problems in the extended SUSY models.

Despite of the fact that left handed and right handed fermions are indicated by doublets and singlet, respectively in SM, particles in SUSY can be represented in irreducible particle states so called ‘‘supermultiplets’’ where each supermultiplet contains

both fermionic and bosonic states with the condition that fermionic and bosonic degree of freedom of each supermultiplet must be equal to each other.

$$n_F = n_B \quad (3.7)$$

where the fermionic and bosonic degrees of freedom in the supermultiplet is represented as  $n_F$  and  $n_B$ , respectively.

In order to construct the SUSY fairly, there are two types of supermultiplets in which each fundamental particle of SM takes part with its corresponding superpartner.

**Chiral (Matter) Supermultiplets** : A chiral supermultiplet consists of a two component chiral Weyl fermion and its corresponding superpartner as a complex scalar field. Since a two component spinor has two degree of freedom on-shell, its corresponding superpartner must be complex scalar field to satisfy the equality of number of degree of freedom in supermultiplets. Chiral supermultiplets classify fermions whose left-handed parts transform differently than the right-handed parts under  $SU(2)_L \times U(1)_Y$ , Higgs bosons and their fermionic superpartners higgsinos. Since there must be one chirality in the SUSY, instead of introducing right handed particles, conjugates of the right handed particles and corresponding right handed superpartners are included in supermultiplets.

**Gauge (Vector) Supermultiplets** : Vector bosons (spin 1) of SM and their fermionic (spin 1/2) superpartners are combined in one supermultiplet so-called ‘‘gauge (vector) supermultiplets’’. To conserve the equality of number of fermionic and bosonic degrees of freedom, superpartner of massless spin 1 vector boson must be a massless two component spin 1/2 Weyl spinor.

### 3.1.1. The Lagrangian for Non-Interacting Wess-Zumino Model

The most basic supersymmetric lagrangian can be represented with one scalar and one fermion field. The Lagrangian and the transformation of these fields can be given as follows

$$\mathcal{L}_{free} = \partial_\mu \Phi^* \partial^\mu \Phi + \Psi^\dagger i \bar{\sigma}^\mu \partial_\mu \Psi \quad (3.8)$$

$$\delta \Phi = \epsilon \Psi \quad \delta \Phi^* = \epsilon^\dagger \Psi^\dagger \quad (3.9)$$

$$\delta \Psi_\alpha = \sigma_\mu \epsilon^\dagger \partial^\mu \Phi \quad \delta \Psi_\alpha^\dagger = \epsilon \sigma_\mu \partial^\mu \Phi^* \quad (3.10)$$

Since the dimension of the scalar field is equal to 1 and the fermion field has dimension of  $\frac{3}{2}$ , the dimension of infinitesimal SUSY parameter  $\epsilon$  can be found as  $-\frac{1}{2}$ . Moreover, square of this infinitesimal SUSY parameter is equal to zero since it is a Grassman number which obey  $\epsilon_i \epsilon_j = -\epsilon_j \epsilon_i$  relation. Then,  $(\epsilon_i)^2 = 0$  since  $\epsilon_i \epsilon_i = -\epsilon_i \epsilon_i$

### 3.1.2. Introducing F terms and D terms

In West-Zumino model, SUSY algebra is not close off-shell. As we stated before, SUSY requires the number of bosonic and fermionic degrees of freedom to be equal in supermultiplets. As a Weyl spinor has two complex components, it has four degree of freedom. However, in case of on-shell fields, the equation of motion imposes two constraints which reduce the number of degree of freedom into two. Since a complex scalar field has two degrees of freedom, the number of fermionic and bosonic degrees of freedom match on-shell. On the other hand, off-shell fields do not have to satisfy the equation of motion and so the number of bosonic and fermionic degrees of freedom do not match. Therefore, SUSY algebra only closes on-shell in case of having a single complex scalar field and a Weyl spinor in theory.

SUSY can be rendered a symmetry also in the off-shell cases by adding scalar “auxiliary field” denoted by  $F$ . Such a field provides two more bosonic off-shell degree of freedom. On the other hand, it does not have a kinetic term, it has to be zero on-shell in a model which is invariant under SUSY transformations. The degrees of freedom of the fields are listed in Table 3.1.

	on-shell	off-shell
$\Phi$	2	2
$\Psi$	2	4
$F$	0	2

Table 3.1. Number of bosonic and fermionic degrees of freedom in Chiral Lagrangian

In order to get the field  $F$  to have no on-shell degrees of freedom, the equation of motion for this field is written as  $F^* = F = 0$ . Since the simplest real term depending on  $F$  and  $F^*$  is  $FF^*$ , Lagrangian takes the form as represented in Eq 3.11.

$$\mathcal{L} = \partial_\mu \Phi^* \partial^\mu \Phi + \Psi^\dagger i \bar{\sigma}^\mu \partial_\mu \Psi + FF^* \quad (3.11)$$

Despite of being a scalar field, dimension of field F is 2, that is,  $[F]=2$ .

$$[\Phi] = 1 \quad [\Psi] = 3/2 \quad [F] = 2$$

After adding F field in our theory, variation of each field can be represented as follows:

$$\delta\Phi = \epsilon\Psi \quad (3.12)$$

$$\delta\Psi = -i\sigma^\mu(i\sigma^2\epsilon^*)\partial_\mu\Phi + F\epsilon \quad (3.13)$$

$$\delta F = -i\epsilon^\dagger\bar{\sigma}^\mu\partial_\mu\Psi \quad (3.14)$$

In order to have a interacting supersymmetric theory, one also has to deal with supersymmetric gauge theories. If we consider U(1) free gauge theory, the superpartner of the photon field  $A_\mu$  will be a left-chiral Weyl spinor denoted by  $\lambda$  and called ‘‘photino’’. Therefore, summation of kinetic terms for the photon and the photino constitute the gauge Lagrangian represented in Eq. 3.15

$$\mathcal{L} = -\frac{1}{4}F_{\mu\nu}F^{\mu\nu} + \lambda^\dagger i\bar{\sigma}^\mu\partial_\mu\lambda \quad (3.15)$$

where transformation of the fields are described as follows

$$\delta A^\mu = \epsilon^\dagger\bar{\sigma}^\mu\lambda + \lambda^\dagger\bar{\sigma}^\mu\epsilon \quad (3.16)$$

$$\delta\lambda = \frac{i}{2}F_{\mu\nu}\sigma^\mu\bar{\sigma}^\nu\epsilon \quad \delta\lambda^\dagger = -\frac{i}{2}F_{\mu\nu}\epsilon^\dagger\bar{\sigma}^\nu\sigma^\mu \quad (3.17)$$

However, here again the algebra does not close off-shell. In case of on-shell,  $A_\mu$  has two degrees of freedom as the two transverse polarization states and also photino represented as a left-chiral Weyl fermion has two degrees of freedom on-shell. Nevertheless, when off-shell, a vector field  $A_\mu$  has three degrees of freedom whereas a left-chiral Weyl fermion has four. Therefore, one has to add one extra bosonic degree of freedom in the form of a real scalar field which is conventionally denoted by D as indicated in Table 3.2.

In order to guarantee the field D to have no on-shell degrees of freedom, the equation of motion for this field is written as  $D = 0$ . Like the auxiliary field F, dimension of D field is also 2. Therefore, following term is added to the Lagrangian.

$$\mathcal{L}_{aux} = \frac{1}{2}D^2 \quad (3.18)$$

	on-shell	off-shell
A	2	3
$\lambda$	2	4
D	0	1

Table 3.2. Number of bosonic and fermionic degrees of freedom in Gauge Lagrangian

$$\mathcal{L} = \mathcal{L}_{gauge} + \mathcal{L}_{aux} = -\frac{1}{4}F_{\mu\nu}F^{\mu\nu} + \lambda^\dagger i\bar{\sigma}^\mu \partial_\mu \lambda + \frac{1}{2}D^2 \quad (3.19)$$

Variation of the fields after adding D real scalar field are defined as follows:

$$\delta A^\mu = \epsilon^\dagger \bar{\sigma}^\mu \lambda + \lambda^\dagger \bar{\sigma}^\mu \epsilon \quad (3.20)$$

$$\delta \lambda = \frac{i}{2}F_{\mu\nu}\sigma^\mu\bar{\sigma}^\nu\epsilon + D\epsilon \quad (3.21)$$

$$\delta D = -i\epsilon^\dagger \bar{\sigma}^\mu \partial_\mu \lambda + i(\partial_\mu \lambda)^\dagger \bar{\sigma}^\mu \epsilon \quad (3.22)$$

### 3.1.3. Superpotential

So far we have considered all the fields are massless and there are no interaction at all. In order to acquire mass to the particles and their superpartners and to make an interacting theory for chiral superfields by describing interactions between the Higgs fields and the matter fields as Higgs field interacts with chiral fields of SM via Yukawa interactions, an analytic function which is called ‘‘superpotential’’ can be proposed as

$$W(\hat{\Phi}) = a\hat{\Phi} + b\hat{\Phi}^2 + c\hat{\Phi}^3 \quad (3.23)$$

where  $\hat{\Phi}$  stands for a chiral superfields. Mass dimensions of the parameters a,b,c are given as [a]= 2, [b]= 1, [c]= 0. Scalar potential of superfields can be obtained from superpotential. In addition to being an analytic function, superpotential is also a holomorphic function which I will refer this property of superpotential in discussing the Higgs sector of MSSM and BLSSM in section 3.2 and subsection 4.1.1. Interaction lagrangian can be written in terms of superpotential as follows



$$\mathcal{L}_{int} = \left( W^i F_i - \frac{1}{2} W^{ij} \Psi_i \Psi_j \right) + h.c \quad (3.24)$$

where  $W$  is superpotential introduced in Eq. 3.25 and  $W^i$  and  $W^{ij}$  are the first and second derivatives of the superpotential with respect to scalar components of the superfields as indicated in Eq 3.26 and Eq 3.27.

$$W = \frac{1}{2} M^{ij} \Phi_i \Phi_j + \frac{1}{6} \Phi_i \Phi_j \Phi_k \quad (3.25)$$

$$W^i = \frac{\partial}{\partial \Phi_i} W \quad (3.26)$$

$$W^{ij} = \frac{\partial^2}{\partial \Phi_i \partial \Phi_j} W \quad (3.27)$$

Total chiral lagrangian can be described as follows

$$\mathcal{L}_{chiral} = \mathcal{L}_{free} + \mathcal{L}_{int} \quad (3.28)$$

$$\mathcal{L} = \partial^\mu \Phi^{*i} \partial_\mu \Phi_i + i \Psi^{\dagger i} \bar{\sigma}^\mu \partial_\mu \Psi_i + F^{*i} F_i + \left( \frac{\partial W}{\partial \Phi_i} F_i - \frac{1}{2} \frac{\partial^2 W}{\partial \Phi_i \partial \Phi_j} \Psi_i \cdot \Psi_j + h.c. \right) \quad (3.29)$$

The equation of motion for the auxiliary field  $F$  gives

$$\frac{\partial \mathcal{L}}{\partial F_i} = 0 \longrightarrow F^{*i} = - \frac{\partial W}{\partial \Phi_i} = -W^i \quad (3.30)$$

$$\frac{\partial \mathcal{L}}{\partial F^{*i}} = 0 \longrightarrow F_i = - \frac{\partial W^*}{\partial \Phi^{*i}} = -W_i^* \quad (3.31)$$

Then, we can represent the terms below

$$F^{*i} F_i + \left( \frac{\partial W}{\partial \Phi_i} \right) F_i + \left( \frac{\partial W^*}{\partial \Phi^{*i}} \right) F^{*i} = - \left| \frac{\partial W}{\partial \Phi_i} \right|^2 \quad (3.32)$$

Therefore, we can express all the chiral lagrangian with independent of  $F$  field as indicated in Eq 3.33

$$\mathcal{L} = \partial^\mu \Phi^{*i} \partial_\mu \Phi_i + i \Psi^{\dagger i} \bar{\sigma}^\mu \partial_\mu \Psi_i - \left| \frac{\partial W}{\partial \Phi_i} \right|^2 - \frac{1}{2} \left( \frac{\partial^2 W}{\partial \Phi_i \partial \Phi_j} \Psi_i \cdot \Psi_j + h.c. \right) \quad (3.33)$$

where the scalar potential is introduced in terms of superpotential as follow

$$V(\Phi_i) = \left| \frac{\partial W}{\partial \Phi_i} \right|^2 \quad (3.34)$$

### 3.1.4. SUSY Breaking

Supercharges commute with the momentum operator as indicated in Eq. 3.35. So, when supercharges is acted on a state, the eigenvalue of  $P^\mu P_\mu$  remains unchanged as in the following.

$$[P_\mu, Q_\alpha] = 0 \quad (3.35)$$

$$\begin{aligned} P^\mu P_\mu |\Psi\rangle &= m^2 |\Psi\rangle \\ Q_\alpha |\Psi\rangle &= m^2 |\Psi\rangle \end{aligned} \quad (3.36)$$

Therefore, all the particles in the same supermultiplet have the same mass. However, if the bosonic partner of electron, so the-called selectron, had exactly the same mass, this would mean that electron could decay to the selectron by giving out a virtual photon. Since selectrons are bosons, they are not restricted by Pauli-Exclusion Principle. Therefore, all selectron could be located in ground state and this would be totally disaster. Fortunately, this kind of particle degeneracy does not exist in nature.

SUSY can be broken by adding some terms to the Lagrangian which are not invariant under SUSY transformations. However, SUSY breaking interactions leads to lost the cancellation of divergences which is the main motivation of SUSY. Therefore, only softly-broken terms are included into the Lagrangian as in Eq. 3.37 in order to keep main motivation of SUSY.

$$\begin{aligned} \mathcal{L}_{\text{SUSY}} &= -\frac{1}{2}(M_1 \tilde{B}\tilde{B} + M_2 \tilde{W}\tilde{W} + M_3 \tilde{g}\tilde{g}) + \text{h.c.} \\ &\quad -m_{H_u}^2 H_u^\dagger H_u - m_{H_d}^2 H_d^\dagger H_d - (bH_u H_d + \text{h.c.}) \\ &\quad -m_Q^2 \tilde{q}^\dagger \tilde{q} - m_L^2 \tilde{l}^\dagger \tilde{l} - m_u^2 \tilde{u}_R^\dagger \tilde{u}_R - m_d^2 \tilde{d}_R^\dagger \tilde{d}_R - m_e^2 \tilde{e}_R^\dagger \tilde{e}_R \\ &\quad - (A_u \tilde{u}_R \tilde{q} H_u + A_d \tilde{d}_R \tilde{q} H_d + A_e \tilde{e}_R \tilde{l} H_d) \end{aligned} \quad (3.37)$$

To break supersymmetry, spontaneous symmetry breaking (SSB) can also be used as another method as we used in SM. In case of SSB, charges that generate the symmetry do not annihilate the ground state.

$$Q|0\rangle \neq 0 \quad (3.38)$$

In SUSY, supercharges  $Q_1$  and  $Q_2$  do not annihilate the ground state. Then, non-zero VEV of the Hamiltonian is obtained.

$$\langle 0|H|0\rangle > 0 \quad (3.39)$$

In free space, kinetic energy part of the Hamiltonian can be taken as zero which leaves us only potential energy part. Since scalar field is the only field that has non-zero VEV, we come up with

$$\langle 0|V(\phi)|0\rangle > 0 \quad (3.40)$$

The auxiliary fields yield the potential energy as in the following.

$$V(\phi_i) = F_i F_i^\dagger + \frac{1}{2} D^2 \quad (3.41)$$

where  $F_i = \frac{\partial W}{\partial \phi_i}$  and  $D = q_i \phi_i^\dagger \phi_i - \xi$  for abelian gauge theories. In this case, a term  $\xi D$  so-called Fayet-Illiopoulos term is included to the Lagrangian. This term is important for D-type SUSY breaking. However, gauge invariance prevents to write a Fayet-Illiopoulos term for non-abelian theories and  $D^a D^a$  term is included to the Lagrangian where  $D^a = g \phi_i^\dagger T^a \phi_i$ .

## 3.2. MSSM

Since they have the same gauge group  $SU(3)_C \times SU(2)_L \times U(1)_Y$ , Minimal Supersymmetric Standard Model (MSMM) which is the minimal extension of the SM is the simplest N=1 supersymmetric model. Each gauge field and each fermion is replaced by a vector supermultiplet and a chiral supermultiplet, respectively. Therefore, MSSM has minimal number of superpartners and their interactions. Since there is a corresponding superpartner for each SM particle, MSSM doubles the number of particles of SM. While SM has one Higgs doublet, for some reason that I explain below, there is an extra doublet Higgs field in MSSM as demonstrated in Eq. 3.42. In SM while d-type quark masses are gained by complex scalar Higgs field itself, charge conjugate of the Higgs field is

introduced to acquire mass to the u-type quarks. However, as it is discussed in subsection 3.1.3, holomorphy feature of superpotential strictly prohibits any field and complex conjugate of that field to exist in the superpotential simultaneously. Since introducing complex conjugate of Higgs field is not allowed in superpotential, one Higgs doublet is not adequate to give mass to all particles as we did in SM. Because of the fact that Yukawa interaction terms can be obtained only from superpotential, second doublet Higgs field is required in the MSSM as represented in Eq. 3.42. To conserve hypercharge, second Higgs doublet ( $H_d$ ) is introduced by assigning -1 hypercharge ( $Y_{H_u} = +1$  and  $Y_{H_d} = -1$ ).

$$H_u = \begin{pmatrix} H_u^+ \\ H_u^0 \end{pmatrix} \quad H_d = \begin{pmatrix} H_d^0 \\ H_d^- \end{pmatrix} \quad (3.42)$$

Superpotential for MSSM is stated by

$$\hat{W} = \mu \hat{H}_u \cdot \hat{H}_d + h_u \hat{Q} \cdot \hat{H}_u \hat{u}_R^c + h_d \hat{Q} \cdot \hat{H}_d \hat{d}_R^c + h_e \hat{L} \cdot \hat{H}_d \hat{e}_R^c \quad (3.43)$$

where  $H_u$ ,  $H_d$ ,  $Q$ ,  $L$ ,  $u_R^c$ ,  $d_R^c$ ,  $e_R^c$  denote the superfields and  $h_u$ ,  $h_d$ ,  $h_e$  stands for dimensionless yukawa couplings. The dot product in the superpotential can be expressed with antisymmetric parameter  $\epsilon^{\alpha\beta}$  such as  $\mu \hat{H}_u \cdot \hat{H}_d = \mu \epsilon^{\alpha\beta} (H_u)_\alpha (H_d)_\beta$ . Instead of antisymmetric parameter  $\epsilon^{\alpha\beta}$ ,  $\mu \hat{H}_u \cdot \hat{H}_d = \mu \hat{H}_u^T (i\sigma_2) \hat{H}_d$  can be used as a another notation.

### 3.2.1. R-parity

In addition to conservation of hypercharge, baryon and lepton number are also conserved in Eq. 3.43. However, it is possible to add some gauge invariant extra terms into superpotential as represented in Eq. 3.44. Even though hypercharge is conserved in these terms and they are not restricted by gauge invariance and renormalization, these extra terms in Eq. 3.44 violate baryon and lepton number conservation.

$$\hat{W}' = \mu' \hat{L} \cdot \hat{H}_u + \lambda_1 \hat{L} \cdot \hat{L} \hat{e}_R^c + \lambda_2 \hat{L} \cdot \hat{Q} \hat{d}_R^c + \lambda_3 \hat{u}_R^c \hat{d}_R^c \hat{d}_R^c \quad (3.44)$$

where the lepton numbers are  $L = +1$  for  $\hat{L}_i$ ,  $L = -1$  for  $\hat{e}_R^c$  and  $L = 0$  for all other supermultiplets and  $B = +1/3$  for  $\hat{Q}_i$ ,  $B = -1/3$  for  $\hat{u}_R^c$ ,  $\hat{d}_R^c$  and  $B = 0$  for all others. Therefore, the first three terms in Eq. 3.44 violates conservation of lepton number by 1 unit and the last term in Eq. 3.44 violates the conservation of baryon number by 1 unit. However, baryon and lepton number violating processes have not been observed in experiments. Besides, if these violating terms are allowed, then proton, which constitutes

the matter, decays rapidly. Proton decay through  $\tilde{s}_R^*$  interaction is represented in Fig. 3.1. Therefore, a new symmetry so-called ‘‘R-parity’’ is introduced to prohibit rapid proton decays and to make it a stable particle.

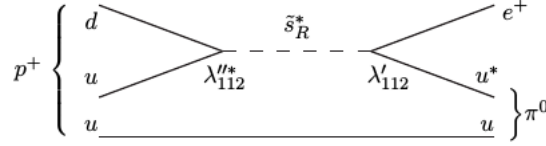


Figure 3.1. Proton decays via R-parity violating  $\tilde{s}_R^*$  interaction

R-parity is defined by introducing opposite R-parity number to the scalar and fermion components of a chiral superfield as follows:

$$P_R = (-1)^{3B+L+2S} \quad (3.45)$$

where B, S and L denotes baryon number, spin and lepton number, respectively.

R-parity introduces opposite R-parity number to the scalar and fermion components of a chiral superfield due to the spin dependence as  $(-1)^{2S}$ . Considering the dependence on the baryon and lepton numbers, all SM particles and the Higgs bosons have  $P_R = +1$  while all superpartners have  $P_R = -1$ . Since this new symmetry is not conserved in Eq 3.44, these interactions become strictly prohibited and proton keeps its stability safely.

R-parity brings two significant results that I remark below

- Since the initial state in the LHC experiments involve only with the SM particles ( $P_R = +1$ ), the conservation of R-parity allows only the processes whose final states include even number of superpartners ( $P_R = -1$ ).

- In the decay chain of a superpartner, lightest supersymmetric particle (LSP) which cannot decay into a SM particle in the final state due to conservation of R-parity must be a stable particle. So, at least one sparticle must be existed as LSP in the final state. If LSP is neutral, it could be evaluated for non-baryonic dark matter candidate.

### 3.3. Successes and Problems of the MSSM

MSSM is firstly introduced to solve the gauge hierarchy problem by stabilizing the Higgs sector which suffers from contributions coming from quantum corrections. In addition to its success in stability of Higgs sector, unifying there gauge couplings in high energies so-called “Grand Unification Scale” provides extra motivation to MSSM.

In SM, gauge couplings of electromagnetic, weak and strong forces do not unify in high energy scales as shown in Figure 3.2. However, MSSM has an energy scale at which three gauge couplings has the same strength. In Figure 3.2, while X axis represents

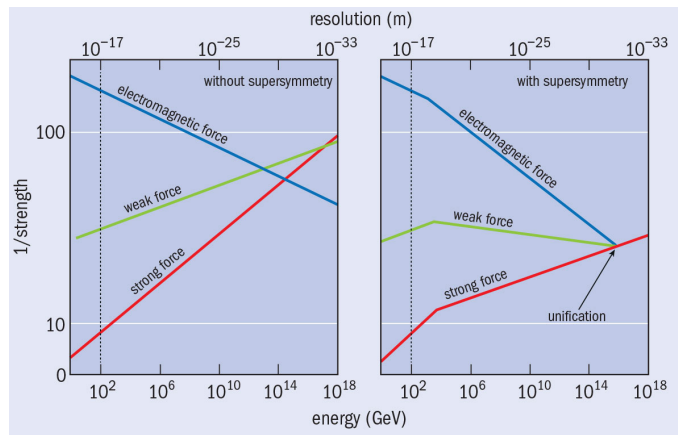


Figure 3.2. Evaluation of gauge couplings in SM (left) and MSSM (right)

the mass or energy on logarithmic scale, Y axis shows 1/strength in terms of fine-structure constant which is linked into square of the corresponding gauge coupling constant.

R-parity and additional particle content of MSSM provide a strong motivation for dark matter problem of SM. As discussed in section 2.2, even though SM explains all the observed particles and their interactions with great precision, these particles correspond to small fraction of total matter in the universe. Dark matter which composes 23% of the observable universe remains unexplained in SM. As result of R-parity, if lightest supersymmetric particle (LSP) is neutral and colorless such as neutralino, sneutrino and gravitino, it cannot take part in electromagnetic and strong interactions. Therefore MSSM could represent its lightest supersymmetric particle (LSP) as a candidate for the dark matter.

Since sparticles are not observed in experiments in the same energy level of their corresponding SM particles, it is sure that SUSY should be a broken symmetry. In order

to cancel one loop radiative correction from the top quark, corresponding top squark mass should be around 1 TeV. Therefore, soft SUSY breaking scale must be above electroweak scale. Although this rescaling creates gauge hierarchy problem one more time, the required fine-tuning is not so much. In this way, MSSM reduces gauge hierarchy problem of SM to “little hierarchy problem”.

One of the most important problem of the MSSM is the  $\mu$  problem. The bi-linear mixing of the MSSM Higgs doublets are characterized with the  $\mu$ -term in the superpotential, and this term is crucial in the electroweak symmetry breaking (EWSB). In this context, EWSB condition can determine the value for  $\mu$ -term up to its sign. Despite its connection to EWSB,  $\mu$ -term can be at any scale, since it preserves SUSY. This is called  $\mu$ -problem in MSSM.

### 3.3.1. Higgs Boson Excesses in CMS

In addition to the problem discussed above, detailed analyses have revealed some anomalies in decay channels of the Higgs boson. While combination of all decay channels excludes the range  $\sim 150 < m_h < 1000$  GeV [11], there is an excess in  $h \rightarrow \gamma\gamma$  at  $m_{\gamma\gamma} \approx 137$  GeV, in addition to that observed at  $m_{\gamma\gamma} \approx 125$  GeV [12]. Similarly,  $h \rightarrow 4l$  exhibits an excess at around  $m_{4l} \approx 146$  GeV [13].

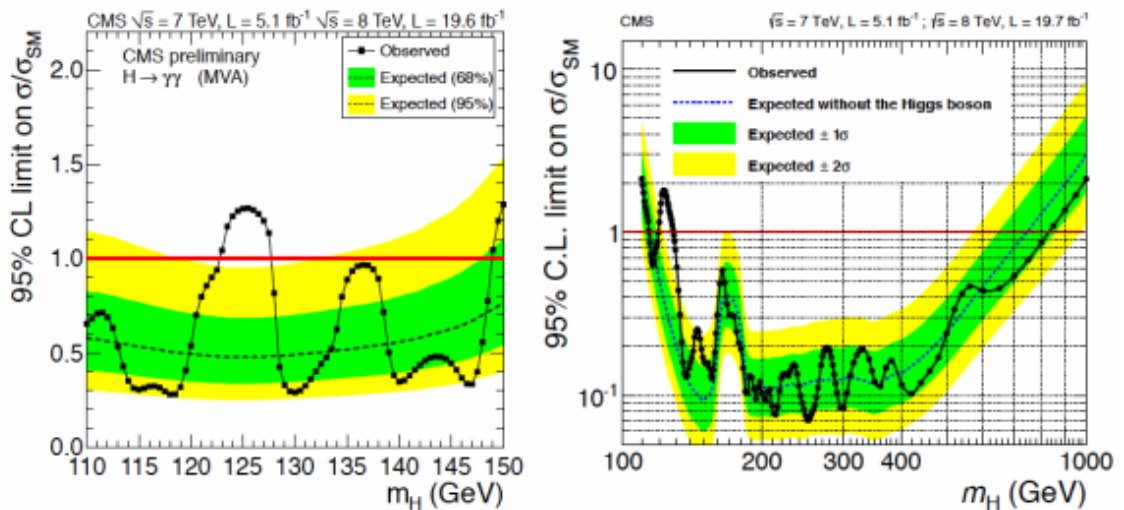


Figure 3.3. CMS data for Higgs boson decays to two photons and Higgs boson decays to four leptons

Figure 3.3 displays the cross-sections of  $h \rightarrow \gamma\gamma$  and  $h \rightarrow ZZ \rightarrow l^+l^-l^+l^-$  decay channels normalized to the SM prediction. CMS data for  $h \rightarrow \gamma\gamma$  and  $h \rightarrow ZZ \rightarrow l^+l^-l^+l^-$  decay channels have revealed excesses at 125 GeV as illustrated in Figure 3.3.

Even though MSSM predicts five physical Higgs bosons, they are quite heavy (generally  $> 500$  GeV) if one considers SUSY GUT models in which an underlying GUT gauge group breaks into the MSSM at the GUT scale. Figure 3.4 illustrates the mass relation between MSSM Higgs bosons. The excess in  $h \rightarrow \gamma\gamma$  channel (left) cannot be accommodated in SUSY GUT models with universal boundary conditions [24]. Moreover, the peak at about 135 GeV requires extra Higgs bosons in addition to those in MSSM. Similarly, in CMS data of higgs boson decaying to four lepton via two Z bosons as shown in Fig.3.3 (right), the first peak at 125 GeV can be explained with the SM Higgs boson. However, the excess at about 145 GeV cannot be explained with the Higgs bosons in minimal SUSY GUT models.

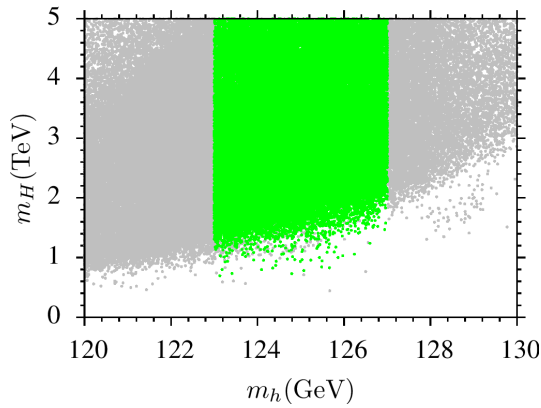


Figure 3.4. Mass of the second lightest Higgs boson vs mass of the SM-like Higgs boson in MSSM



# CHAPTER 4

## B-L SYMMETRIC SSM

### 4.1. $U(1)_{B-L}$ Extention of MSSM

Some of the terms in the MSSM superpotential violates lepton or baryon number which lead to the unobserved rapid proton decay. One possible solution to this problem is to define a new symmetry so-called R-parity under MSSM gauge group as discussed in subsection 3.2.1. Since the attempts to explain R-parity in MSSM require some assumptions, these are all “non-minimal” solutions. When the minimality discussion is taken into consideration, MSSM may not cover the full story and one may consider some extensions of the MSSM gauge group. One of the simplest extension of MSSM gauge group can be constructed by imposing an extra  $U(1)$  group. Such an extension can be obtained from the underlying GUT theories including a gauge group larger than  $SU(5)$  [21]. Among the many different  $U(1)$  extensions,  $U(1)_{B-L}$  can be preferred since anomaly cancellations are achieved by adding three MSSM singlet and R-parity arises in a natural way if the MSSM is invariant under a global  $U(1)_{B-L}$  symmetry. Right-handed neutrino can be considered for these MSSM singlet fields. In this way, non-zero neutrino masses [22] can be acquired through different see-saw mechanisms in anomaly free  $U(1)_{B-L}$  extention of MSSM. In the type-I seesaw mechanism, Majorana mass term is not allowed till B-L symmetry gets broken. After B-L symmetry breaking, the right handed neutrinos acquire their Majorana masses. Moreover, R-parity which we define to avoid rapid proton decay by demanding the MSSM gauge group to be invariant under  $Z_4$  symmetry must also be imposed again with the  $U(1)_{B-L}$  extension. Fortunately, smallness of the neutrino masses do not allow the R-parity violation. Besides, R-parity conservation continues even after  $U(1)_{B-L}$  symmetry breaking [23].  $U(1)_{B-L}$  symmetry can be broken radiatively through a similar mechanism to the radiative electroweak symmetry breaking (REWSB) of MSSM [25]. A proposed field which has non-zero vacuum expectation value (VEV) break the  $U(1)_{B-L}$  symmetry. Besides, this field has to carry non-zero B-L charge and it should preferably be singlet in order not to break MSSM gauge symmetry. If B-L charge of this proposed singlet particle is 2, then the R-parity conservation can be sustained. Because

of the holomorphy feature of the superpotential, another singlet field with B-L charge -2 is required to construct an invariant lagrangian under  $U(1)_{B-L}$  gauge group. In this way,  $U(1)_{B-L}$  extension of MSSM (BLSSM) proposes two new singlet Higgs fields  $\mathcal{X}_1$  and  $\mathcal{X}_2$  whose B-L charges are +2 and -2, respectively. These new singlet Higgs fields can accomodate to the observed Higgs decay excesses at the mass scales other than  $\sim 125$  GeV. In the rest of this chapter, we briefly describe the model by emphasizing the Higgs sector of BLSSM.

Names	Superfields	Spin 0	Spin 1/2	$SU(3)_C$ , $SU(2)_L$ , $U(1)_Y$ , $U(1)_{B-L}$
Squarks, Quarks	$\widehat{Q}_i$	$(\widetilde{u}_{L_i} \widetilde{d}_{L_i})$	$(u_{L_i} d_{L_i})$	$(3, 2, \frac{1}{6}, \frac{1}{3})$
	$\widehat{u}_{R_i}^c$	$\widetilde{u}_{R_i}^*$	$u_{R_i}^\dagger$	$(\bar{3}, 1, \frac{2}{3}, \frac{1}{3})$
	$\widehat{d}_{R_i}^c$	$\widetilde{d}_{R_i}^*$	$d_{R_i}^\dagger$	$(\bar{3}, 1, -\frac{1}{3}, \frac{1}{3})$
Sleptons, Leptons	$\widehat{L}_i$	$(\widetilde{\nu}_{L_i} \widetilde{e}_{L_i})$	$(\nu_{L_i} e_{L_i})$	$(1, 2, -\frac{1}{2}, -1)$
	$\widehat{e}_{R_i}^c$	$\widetilde{e}_{R_i}^*$	$e_{R_i}^\dagger$	$(1, 1, -1, -1)$
	$\widehat{N}_i^c$	$\widetilde{N}_i^*$	$N_i^\dagger$	$(1, 1, 0, -1)$
Higgs, Higgsinos	$\widehat{H}_u$	$(H_u^+ H_u^0)$	$(\widetilde{H}_u^+ \widetilde{H}_u^0)$	$(1, 2, \frac{1}{2}, 0)$
	$\widehat{H}_d$	$(H_d^0 H_d^-)$	$(\widetilde{H}_d^0 \widetilde{H}_d^-)$	$(1, 2, -\frac{1}{2}, 0)$
	$\widehat{\mathcal{X}}_1$	$\mathcal{X}_1^0$	$\widetilde{\mathcal{X}}_1$	$(1, 1, 0, -2)$
	$\widehat{\mathcal{X}}_2$	$\mathcal{X}_2^0$	$\widetilde{\mathcal{X}}_2$	$(1, 1, 0, +2)$

Table 4.1. Chiral (Matter) Supermultiplets in the BLSSM

Names	Superfields	Spin 1/2	Spin 1	$SU(3)_C$ , $SU(2)_L$ , $U(1)_Y$ , $U(1)_{B-L}$
Gluino, Gluons	$\widehat{G}$	$\widetilde{g}$	$\mathbf{g}$	$(8, 1, 0, 0)$
Winos, W bosons	$\widehat{W}$	$\widetilde{W}^\pm, \widetilde{W}^0$	$W^\pm, W^0$	$(1, 3, 0, 0)$
Bino, B boson	$\widehat{B}$	$\widetilde{B}^0$	$B^0$	$(1, 1, 0, 0)$
$B'$ -ino, $B'$ boson	$\widehat{B}'$	$\widetilde{B}'^0$	$B'^0$	$(1, 1, 0, 0)$

Table 4.2. Gauge (Vector) Supermultiplets in the BLSSM

### 4.1.1. Model Description

In this section, we will describe BLSSM with the gauge group

$$SU(3)_C \otimes SU(2)_L \otimes U(1)_Y \otimes U(1)_{B-L} \quad (4.1)$$

The superpotential of the BLSSM is given in the following way.

$$\begin{aligned} W = & \mu H_u H_d + Y_u^{ij} Q_i H_u u_j^c + Y_d^{ij} Q_i H_d d_j^c + Y_e^{ij} L_i H_d e_j^c \\ & + Y_\nu^{ij} L_i H_u N_j^c + Y_N^{ij} N_i^c N_j^c \mathcal{X}_1 + \mu' \mathcal{X}_1 \mathcal{X}_2 \end{aligned} \quad (4.2)$$

where the terms in the first line are associated with MSSM superpotential while the terms in the second line stand for the interaction between neutrinos and the doublet Higgs fields, Majorana interactions for the neutrinos and the interaction between singlet Higgs fields, respectively. Since BLSSM includes right-handed neutrinos, a term describing neutrino interactions is allowed to write into the superpotential. The coupling of this term  $Y_\nu$  is defined as Yukawa coupling for neutrinos. In a similar way, the interaction between right-handed neutrinos and singlet Higgs boson  $\mathcal{X}_1$  is determined by  $Y_N$  yukawa coupling. Finally, the last term in the BLSSM superpotential stands for bilinear mixing of the singlet Higgs bosons  $\mathcal{X}_1$  and  $\mathcal{X}_2$ . In Non-SUSY version of B-L model, mixing terms for doublet and singlet Higgs fields are allowed in the Lagrangian and Higgs potential ( $\lambda_3 H^\dagger H |\mathcal{X}|^2$ ). However, these mixings terms are not allowed through superpotential in BLSSM. Therefore, Higgs potential of BLSSM does not include any mixing term of these fields. Then, the Higgs potential of doublet Higgs fields and the Higgs potential of singlet Higgs fields can be analysed separately. The Higgs potentials associated with the doublet and singlet Higgs fields are represented in the following way, respectively.

$$V_{BLSSM} = V(H_1, H_2) + V(\mathcal{X}_1, \mathcal{X}_2) \quad (4.3)$$

$$\begin{aligned} V(H_1, H_2) = & \frac{1}{2} g^2 \left( H_1^* \frac{\tau^a}{2} H_1 + H_2^* \frac{\tau^a}{2} H_2 \right)^2 + \frac{1}{8} g^2 (|H_2|^2 - |H_1|^2)^2 \\ & + m_1^2 |H_1|^2 + m_2^2 |H_2|^2 - m_3^2 (H_1 H_2 + h.c.) \end{aligned} \quad (4.4)$$

$$V(\mathcal{X}_1, \mathcal{X}_2) = \mu_1^2 |\mathcal{X}_1|^2 + \mu_2^2 |\mathcal{X}_2|^2 - \mu_3^2 (\mathcal{X}_1 \mathcal{X}_2 + h.c.)$$

$$+\frac{1}{2}g_{BL}^2(|\mathcal{X}_2|^2 - |\mathcal{X}_1|^2)^2 \quad (4.5)$$

where

$$\begin{aligned} m_i^2 &= m_0^2 + \mu^2, \quad i = 1, 2 & m_3^2 &= -B\mu \\ \mu_i^2 &= m_0^2 + \mu'^2, \quad i = 1, 2 & \mu_3^2 &= -B\mu' \end{aligned}$$

and  $g_{BL}$  is the gauge coupling associated with the  $B - L$  gauge group.

Since the singlet Higgs potential is similar to the MSSM Higgs potential, similar equations are obtained as a result of minimization of the singlet Higgs potential. If the same steps in the minimization of MSSM potential are applied, the minimization of  $V(\mathcal{X}_1, \mathcal{X}_2)$  gives the VEV's of  $\mathcal{X}_1$  and  $\mathcal{X}_2$  as follows:

$$v'^2 = (v_1'^2 + v_2'^2) = \frac{(\mu_1^2 - \mu_2^2) - (\mu_1^2 + \mu_2^2)\cos 2\theta}{2g_{BL}^2 \cos 2\theta}$$

where the angle  $\tan\theta = \frac{v_1'}{v_2'}$ . Consequently, when singlet Higgs boson masses  $m_{\mathcal{X}_1}$  or  $m_{\mathcal{X}_2}$  (or both) is negative, the VEV's of the  $\mathcal{X}_1$  and  $\mathcal{X}_2$  correspond a value bigger than zero.

#### 4.1.2. Soft SUSY Breaking in BLSSM

Relevant soft supersymmetry breaking (SSB) Lagrangian is represented as follows:

$$\begin{aligned} -\mathcal{L}_{\text{SUSY}} &= -\mathcal{L}_{\text{SUSY}}^{\text{MSSM}} + m_{\tilde{N}^c}^2 |\tilde{N}^c|^2 + m_{\mathcal{X}_1}^2 |\mathcal{X}_1|^2 + m_{\mathcal{X}_2}^2 |\mathcal{X}_2|^2 \\ &\quad + A_\nu \tilde{L} H_u \tilde{N}^c + A_N \tilde{N}^c \tilde{N}^c \mathcal{X}_1 \\ &\quad + \frac{1}{2} M_{\tilde{B}'} \tilde{B}' \tilde{B}' + B(\mu' \mathcal{X}_1 \mathcal{X}_2 + \text{h.c.}) \end{aligned} \quad (4.6)$$

In addition to the terms associated with the SSB terms of MSSM, extra terms breaking  $U(1)_{B-L}$  symmetry are added to the SSB Lagrangian of BLSSM to break  $U(1)_{B-L}$  symmetry. In Eq. 4.6,  $m_{\tilde{N}^c}$ ,  $m_{\mathcal{X}_1}$  and  $m_{\mathcal{X}_2}$  denote the mass terms for the right-handed sneutrinos and singlet Higgs fields, respectively.  $A_\nu$  term is trilinear scalar interaction of sneutrinos and MSSM Higgs doublet  $H_u$  while  $A_N$  term is trilinear scalar interaction between right-handed sneutrinos and singlet Higgs boson of BLSSM  $\mathcal{X}_1$ . The term,  $M_{\tilde{B}'} \tilde{B}' \tilde{B}'$ , is the mass term for gaugino  $\tilde{B}'$  which corresponds to the superpartner of the gauge boson associated with  $U(1)_{B-L}$  group. In addition to this, there also exists a vector

boson partner  $Z'$ . The experimental bounds constrain the  $Z'$  boson mass to be larger than 2.5 TeV.

When a similar analysis to Radiative Electroweak Symmetry Breaking (REWSB) is conducted, it can be easily seen from the associated renormalization group equation (RGE) that the coupling  $Y_N$  between the right-handed neutrinos and the singlet Higgs boson  $\mathcal{X}_1$  contributes negatively to  $m_{\mathcal{X}_1}^2$  as represented in Eq. 4.7.

$$\frac{dm_{\mathcal{X}_1}^2}{dt} = \frac{1}{16\pi^2} [6g_{BL}M_{BL}^2 - 2Y_N(m_{\mathcal{X}_1}^2 + 2m_N^2 + A_N^2)] \quad (4.7)$$

If  $Y_N$  value is large enough,  $m_{\mathcal{X}_1}^2$  can take negative values which leads to the spontaneous B-L symmetry breaking. However, it turns out that for the larger values of  $Y_N$ , the right-handed sneutrino can develop a non-zero VEV as can be seen from the relevant RGE in Eq. 4.8.

$$\frac{dm_N^2}{dt} = \frac{1}{16\pi^2} \left[ \frac{3}{2}g_{BL}M_{BL}^2 - Y_N(m_{\mathcal{X}_1}^2 + 2m_N^2 + A_N^2) \right] \quad (4.8)$$

As a result, Majorana mass term breaks the R-parity by destabilizing the vacuum [26]. Therefore,  $Y_N$  value should be large enough to break B-L symmetry but small enough not to break R-parity.

### 4.1.3. The Higgs Sector of BLSSM

In this subsection, we will emphasize the Higgs sector of BLSSM. After the spontaneous symmetry breaking, fields mix and construct non-diagonal mass matrices. Since MSSM doublet Higgs bosons and BLSSM singlet Higgs bosons do not mix each other, doublet and singlet Higgs boson sectors can be analysed separately. Since singlet Higgs bosons  $\mathcal{X}_1$  and  $\mathcal{X}_2$  are singlet under MSSM gauge group, they do not couple to MSSM particles at tree-level. However, they can still interact with MSSM particles through loop level.

The Feynman diagrams in Fig. 4.1 represent the interaction between singlet Higgs field and the fermions in loop level. The top diagrams stand for the non-supersymmetric interactions while the below ones illustrate how the singlet Higgs field interact through supersymmetric partners. In Fig. 4.1,  $\tilde{f}$ ,  $\tilde{N}$ ,  $\tilde{\chi}^0$  and  $\tilde{\chi}^\pm$  represent the sfermions, right-handed sneutrinos, neutralinos and charginos, respectively. In the top left diagram, fermions interact with the singlet Higgs boson through  $Z'$  loop. However, this interaction is generally suppressed due to the heavy mass of  $Z'$  ( $m_{Z'} \gtrsim 2.5$  TeV). In the right top and bottom

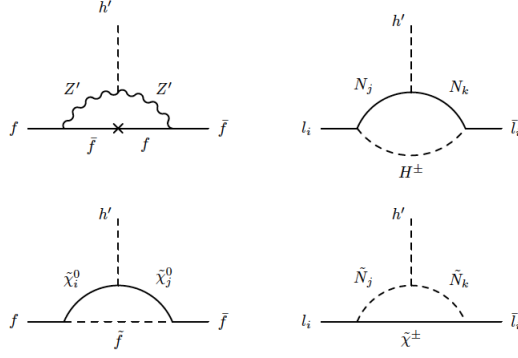


Figure 4.1. The effective Yukawa interactions between the singlet Higgs boson and fermions. The top diagrams illustrate the non-SUSY loops, while the bottom diagrams display the SUSY interference.

diagrams, since there is no interaction between MSSM gauge group and BLSSM singlet Higgs fields, the singlet Higgs fields cannot couple to the left-handed neutrinos at tree level. In these diagrams, the interaction between leptons and the singlet Higgs boson depends on the interaction between right-handed neutrinos, Yukawa coupling of the Majorana mixing  $Y_N$  and the sparticle mass running through the loop. The right below diagram is also generally suppressed due to heavy masses of right-handed sneutrinos (generally at TeV scale). The contribution obtained from left below diagram depends on  $\tilde{B}'$  mass which can be light (about 100 GeV) enough to be LSP since there is no experimental bound on  $\tilde{B}'$  mass [27].

According to the discussion above, even though singlet Higgs boson can join to low scale implications, these contributions obtained from loop order will not be enough to explain the observed decay anomalies in the SM. However, when the mixing term of the  $U(1)$  gauge groups are added into the Lagrangian, new Lagrangian still remains invariant. This mixing is defined with the term  $-\kappa_{ab}B_{\mu\nu}^a B^{b,\mu\nu}$  where  $B_{\mu\nu}$  is the field strength tensor of  $U(1)$  gauge fields,  $a, b = Y, B - L$ , the hypercharge and B-L charge, respectively and  $\kappa_{ab}$  is an antisymmetric tensor which mixes the fields associated with  $U(1)_a$  and  $U(1)_b$  gauge groups. Even if the mixing between the MSSM gauge sector and B-L sector is set to zero at the GUT scale  $M_{\text{GUT}}$ , it can be induced through RGEs at low energy scale [28]. In case of non-zero gauge kinetic mixing, the gauge covariant derivative is defined as follow:

$$\mathcal{D}_\mu = \partial_\mu - i(Y, B - L) \begin{pmatrix} g_Y & \tilde{g} \\ \tilde{g}' & g_{B-L} \end{pmatrix} \begin{pmatrix} B_\mu \\ B'_\mu \end{pmatrix} \quad (4.9)$$

where the fields is declared in the flavour basis. As discussed in [29], the fields can be rotated as illustrated below.

$$\begin{pmatrix} g_Y & \tilde{g} \\ \tilde{g}' & g_{B-L} \end{pmatrix} \rightarrow \begin{pmatrix} g_1 & g_{YB} \\ 0 & g_4 \end{pmatrix}$$

where  $g_1$  stands for the hypercharge coupling associated with the BLSSM,  $g_4$  corresponds to coupling of the B-L charge and  $g_{YB}$  is the coupling related to the mixing of the  $U(1)_Y$  and  $U(1)_{B-L}$  group [29, 30].

When the gauge kinetic mixing is included into the Lagrangian, the contribution obtained from the  $Z'$  loop in the top left diagram starts to be significant. Moreover, gauge kinetic mixing shows its effect in other sectors, as well. Especially, as soon as the gauge mixing is included into the BLSSM, MSSM Higgs doublets and BLSSM Higgs singlets directly interact with each other at tree level. The mixing ratio of the abelian  $U(1)$  gauge groups depends on the coupling  $g_{YB}$ . After the gauge kinetic mixing is allowed and MSSM doublet Higgs bosons and BLSSM singlet Higgs bosons interact with each other, their mass squared matrices should be diagonalized together. As a fact of this, all particles in BLSSM can interact at tree level. In this way, the contributions obtained from the interactions in Fig. 4.1 becomes corrective contribution to tree level interactions. With the BLSSM singlet Higgs bosons which couples to the MSSM particles at tree level, the motivation becomes obtained in order to provide an explanation for the excesses at the scales other than 125 GeV as discussed in previous chapter.

#### 4.1.4. The Right-Handed Neutrino Contribution

As can be seen from the superpotential in Eq. 4.2, there exists a Yukawa term  $Y_\nu^{ij} L_i H_u N_i^c$  so that the right-handed neutrino can interact with MSSM doublet Higgs boson  $H_u$ . This term gives contribution to the SM-like Higgs boson in addition to the contributions from the stop sector; and hence, it can improve the required fine tuning in BLSSM by loosing the mass bound on stop. However, after the electroweak symmetry breaking, this term provides a Dirac mass for neutrinos. The relevant Yukawa coupling  $Y_\nu$  remains to be small ( $Y_\nu \lesssim 10^{-7}$ ) due to the smallness of the neutrino masses [31]. As a result, the contributions to the Higgs boson from the neutrino sector is suppressed by such a small  $Y_\nu$ . Therefore, the low scale Higgs phenomenology of MSSM and BLSSM are similar to each other.  $Y_\nu$  values can be at the order of unity by implementing the inverse see-saw mechanism to BLSSM [32]. With the inverse see-saw mechanism, the

contribution to the Higgs boson from the right-handed neutrinos become unavoidable [33]. In the superpotential of BLSSM with inverse seesaw, there exists a term  $(Y_S \hat{\nu} \hat{\mathcal{X}}_1 \hat{S}_2)$  which the SM singlet Higgs field interacts with the SM singlet chiral superfields [27]. This term increases the masses of the singlet Higgs boson in a substantial amount. Hence, another Higgs boson cannot be accommodated to the mass scale lighter than 150 GeV in BLSSM with inverse seesaw constrained from  $M_{\text{GUT}}$ . In other words, another Higgs boson has to be heavier than 150 GeV in order to be consistent with SM Higgs boson at the mass scale of 125 GeV. Therefore, we did not involve the inverse seesaw mechanism into the BLSSM. However, even if BLSSM is not blended with the inverse seesaw mechanism, the right-handed neutrino sector has significant contribution to the singlet Higgs boson masses due to the Majorana mixing term  $(Y_N^{ij} N_i^c N_j^c \mathcal{X}_1)$  in the superpotential. However, since the SM-like Higgs boson  $H_u$  does not take significant contribution from the right-handed neutrinos through the Yukawa interaction term  $Y_\nu^{ij} L_i H_u N_j^c$ , the singlet Higgs bosons can be light enough in spite of diagonalizing with doublet Higgs fields of MSSM.



# CHAPTER 5

## MASS SPECTRUM AND HIGGS BOSON DECAYS IN BLSSM

This chapter is arranged as follow: After we summarize the scanning procedure and the experimental constraints employed in our analysis in section 5.1, we present our results for the mass spectrum in section 5.2. We also briefly mention about leptogenesis in this section. In section 5.3, we consider the Higgs boson decays into two photons and four leptons. Finally we summarize and conclude the thesis in section ??

### 5.1. Scanning Procedure and the Experimental Constraints

We have employed SPheno 3.3.3 package [34] obtained with SARAH 4.5.8 [35]. In this package, weak scale values of the gauge and Yukawa couplings in MSSM are evolved to the unification scale  $M_{\text{GUT}}$  through RGEs.  $M_{\text{GUT}}$  scale is determined by the requirement of the gauge coupling unification. Since the effective field theory (EFT) is just an approximation of a full theory which is valid at the low energy scale (below some threshold), the threshold corrections should also be calculated or estimated while studying with a GUT theory. If  $A_{\text{eff}}$  is any amplitude calculated with the EFT and  $A_{\text{full}}$  is the amplitude for the same process calculated with the full theory, the threshold correction is defined as  $A_{\text{full}} - A_{\text{eff}}$ . Since a few percent deviation at  $M_{\text{GUT}}$  scale is considered for GUT-scale threshold corrections, we do not strictly enforce the exact unification condition  $g_1 = g_2 = g_3$  at  $M_{\text{GUT}}$  [36]. We rather allow a few percent deviation in  $g_3$  in order to count some unknown threshold corrections at  $M_{\text{GUT}}$ . With the boundary conditions determined at  $M_{\text{GUT}}$  scale, all SSB parameters along with gauge and Yukawa couplings are evolved back to the weak scale. The gauge coupling associated with the  $U(1)_{B-L}$  is determined by a constraint  $g_1 = g_2 = g_4 \approx g_3$ .

The requirement of the radiative electroweak symmetry breaking (REWSB) [37] puts an important theoretical constrain in the parameter space. In addition, B-L symmetry breaking and R-parity conservation constraint rather right-handed neutrino sector and the relevant Yukawa coupling  $Y_N$  as discussed in the subsection 4.1.2. We set  $Y_N = 0.4$  in our work also to avoid the Landau pole while the RGEs are run up to the GUT scale.

We have performed random scans over the following parameter space.

$$\begin{aligned}
0 &\leq m_0 &&\leq 3 \text{ (TeV)} \\
0 &\leq M_{1/2} &&\leq 5 \text{ (TeV)} \\
1.2 &\leq \tan \beta &&\leq 60 \\
-3 &\leq A_0/m_0 &&\leq 3 \\
\mu &> 0, \quad \mu' > 0, \quad m_t = 173.3 \text{ GeV}
\end{aligned} \tag{5.1}$$

In Eq. 5.1,  $m_0$  is the SSB mass term for all scalar fields including the MSSM doublet and BLSSM singlet Higgs fields while  $M_{1/2}$  stands for the SSB mass term for gauginos including the  $B'$  gauge boson corresponding to the  $U(1)_{B-L}$  group. As  $A_0$  represents the SSB trilinear scalar interacting terms,  $\tan \beta$  denotes the ratio of the vacuum expectation values of MSSM Higgs doublets. The ratio of the VEVs of BLSSM singlet Higgs fields is also a free parameter in BLSSM. However, in this work this ratio is constrained at the unity order ( $\tan \beta' \equiv v_{\chi_1}/v_{\chi_2} \approx 1 - 1.2$ ). Moreover, we scan only positive values of  $\mu$  and  $\mu'$  which are bilinear mixing of the MSSM doublet and BLSSM singlet Higgs fields, respectively. Besides, we set the top quark mass  $m_t$  to its central value ( $\approx 173.3$  GeV) [38]. The reason of this is that sparticle masses are not too sensitive to top quark mass [39] while Higgs boson mass can vary approximately 1-2 GeV depending on the top quark mass [40]. Finally, we also vary the coupling  $g_{YB}$  associated with gauge kinetic mixing but fix  $Y_N \approx 0.4$ .

While scanning the parameter space, we use our interface which employs Metropolis-Hasting algorithm as in [41]. All the data points are controlled by SPheno package to satisfy the requirement of REWSB. After the data is collected, the mass bounds for all particles [42] and the following phenomenological constraints are applied.

$$m_h = 123 - 127 \text{ GeV} \quad [3, 4] \tag{5.2}$$

$$m_{\tilde{g}} \geq 1.8 \text{ TeV} \tag{5.3}$$

$$m_{\tilde{\tau}} \geq 105 \text{ GeV} \tag{5.4}$$

$$m_{\tilde{\chi}_1^\pm} \geq 103.5 \text{ GeV} \tag{5.5}$$

$$m_{\tilde{t}_1} \geq 175 \text{ GeV} \tag{5.6}$$

$$0.8 \times 10^{-9} \leq \text{BR}(B_s \rightarrow \mu^+ \mu^-) \leq 6.2 \times 10^{-9} (2\sigma) \tag{5.7}$$

$$2.99 \times 10^{-4} \leq \text{BR}(b \rightarrow s\gamma) \leq 3.87 \times 10^{-4} (2\sigma) \tag{5.8}$$

$$0.15 \leq \frac{\text{BR}(B_u \rightarrow \tau\nu_\tau)_{\text{MSSM}}}{\text{BR}(B_u \rightarrow \tau\nu_\tau)_{\text{SM}}} \leq 2.41 (3\sigma) \tag{5.9}$$

In parameter space, we choose  $\mu > 0$  and  $\mu' > 0$  to force the solutions at least as good as the Standard Model prediction for the muon anomalous magnetic moment [45].

In addition to the constraints mentioned above, another constraint comes from the dark matter (DM) observations. This constraint demands the lightest supersymmetric particle (LSP) stable and of no electric or color charge. However, when this constraint is applied, it significantly limits the parameter space and excludes the regions leading to  $\tilde{\tau}$  or  $\tilde{t}$  LSP solutions. On the other hand, even if a solution is excluded by the DM constraints, such solutions can still survive in some DM scenarios [46]. Therefore, the DM constraints is not implemented in our scan and we do not require the solutions to yield neutralino LSP.

## 5.2. Mass Spectrum

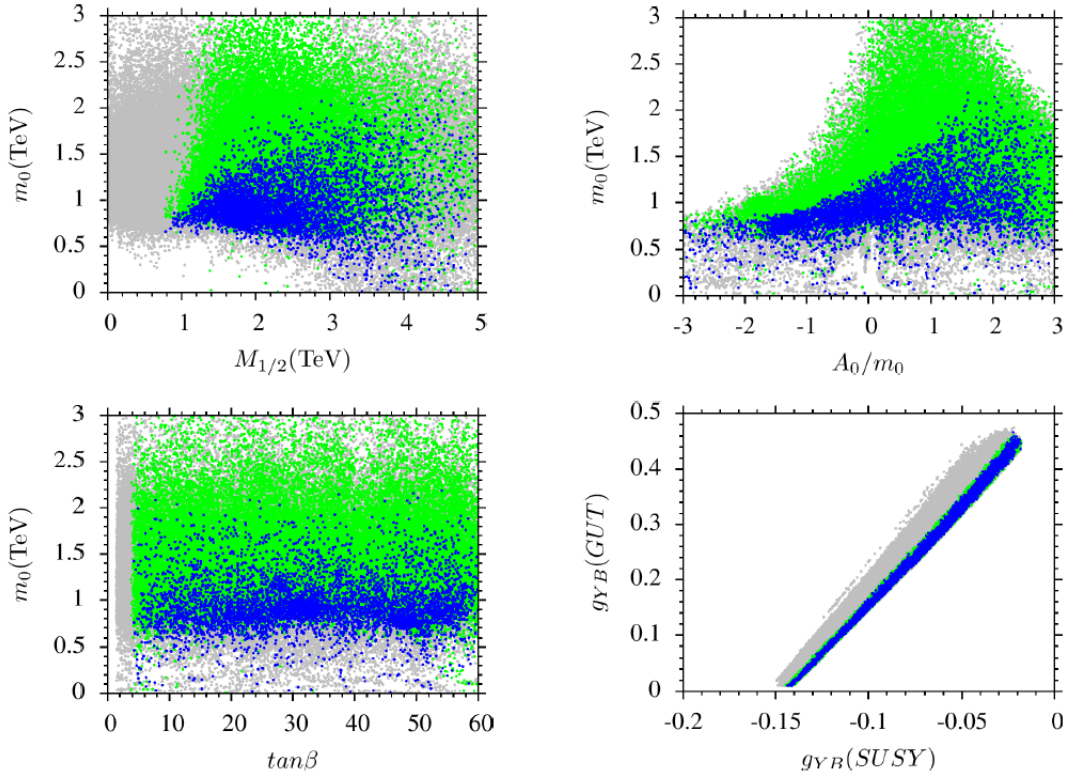


Figure 5.1. Plots in  $m_0 - M_{1/2}$ ,  $m_0 - A_0/m_0$ ,  $m_0 - \tan\beta$ , and  $g_{YB}(GUT) - g_{YB}(SUSY)$  planes. All points are consistent with REWSB. Green points satisfy the mass bounds and the constraints from the rare B-decays. Blue points form a subset of green, and they represent solutions with  $m_{h_2} \leq 150$  GeV.

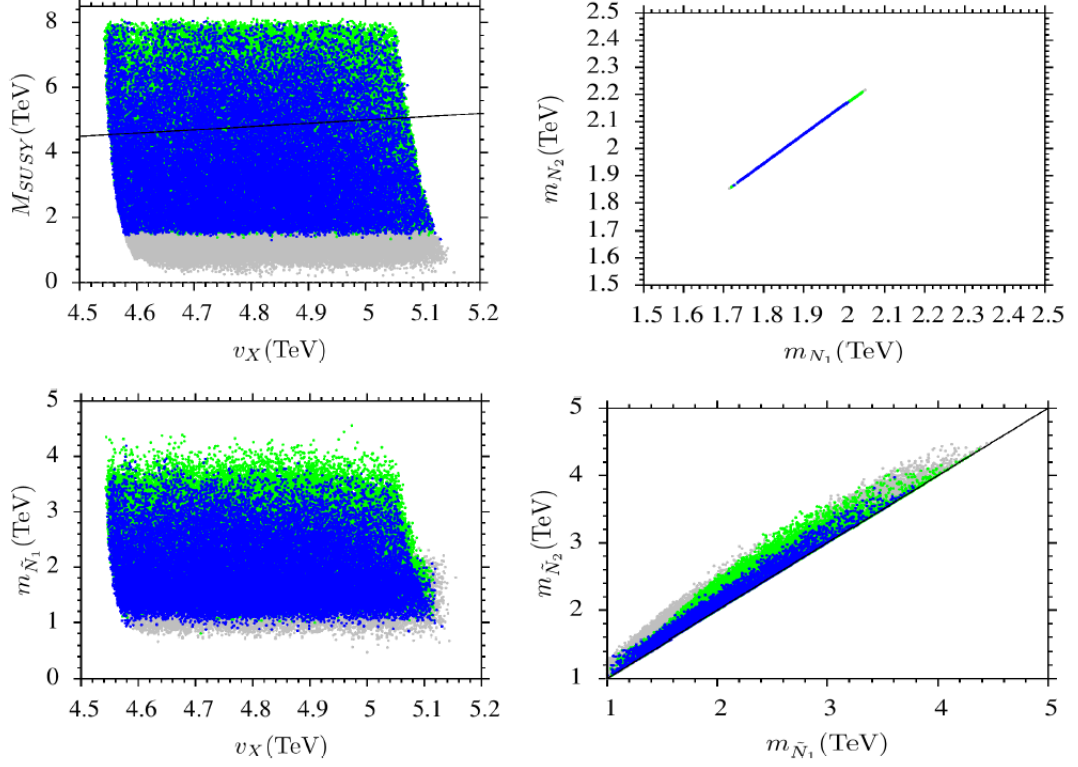


Figure 5.2. Plots in the  $M_{\text{SUSY}} - v_X$ ,  $m_{N_2} - m_{N_1}$ ,  $M_{\tilde{N}_1} - v_X$ , and  $m_{\tilde{N}_2} - m_{\tilde{N}_1}$  planes. The color coding is the same as Figure 5.1. The solid line in the  $M_{\text{SUSY}} - v_X$  plane indicates the regions where  $M_{\text{SUSY}} = v_X$ .

In this section, we present the results for the mass spectrum obtained from the scan over the parameter space given in Eq.(5.1). Figure 5.1 displays the regions with plots in  $m_0 - M_{1/2}$ ,  $m_0 - A_0/m_0$ ,  $m_0 - \tan \beta$ , and  $g_{YB}(\text{GUT}) - g_{YB}(\text{SUSY})$  planes. All points are consistent with REWSB. The solutions which satisfy the mass bounds and the constraints from the rare B-decays are illustrated with green points. Blue points form a subset of green, and they stand for solutions with  $m_{h_2} \leq 150$  GeV. We can easily see from the  $m_0 - M_{1/2}$  plane that the condition for the second Higgs boson lighter than 150 GeV (blue) excludes significant portion of the LHC allowed region (green). For  $M_{1/2} \sim 1$  TeV,  $m_0$  is restricted to a narrow range at about 500 GeV, and this range evolves to 2 TeV for heavier gaugino masses. This relation can be partially understood with the heavy gaugino effect on the singlet Higgs boson mass. Even though we require very light mass range for all scalar particles at the GUT scale, the heavy gaugino masses ( $M_{B-L}$ ) increase the singlet Higgs boson mass such that  $m_{h_2} \lesssim 150$  GeV. On the other hand, large values of  $m_0$  correspond to heavy  $m_{\chi_1}$  and  $m_N$ . As can be seen from Eq.(4.7), larger values of

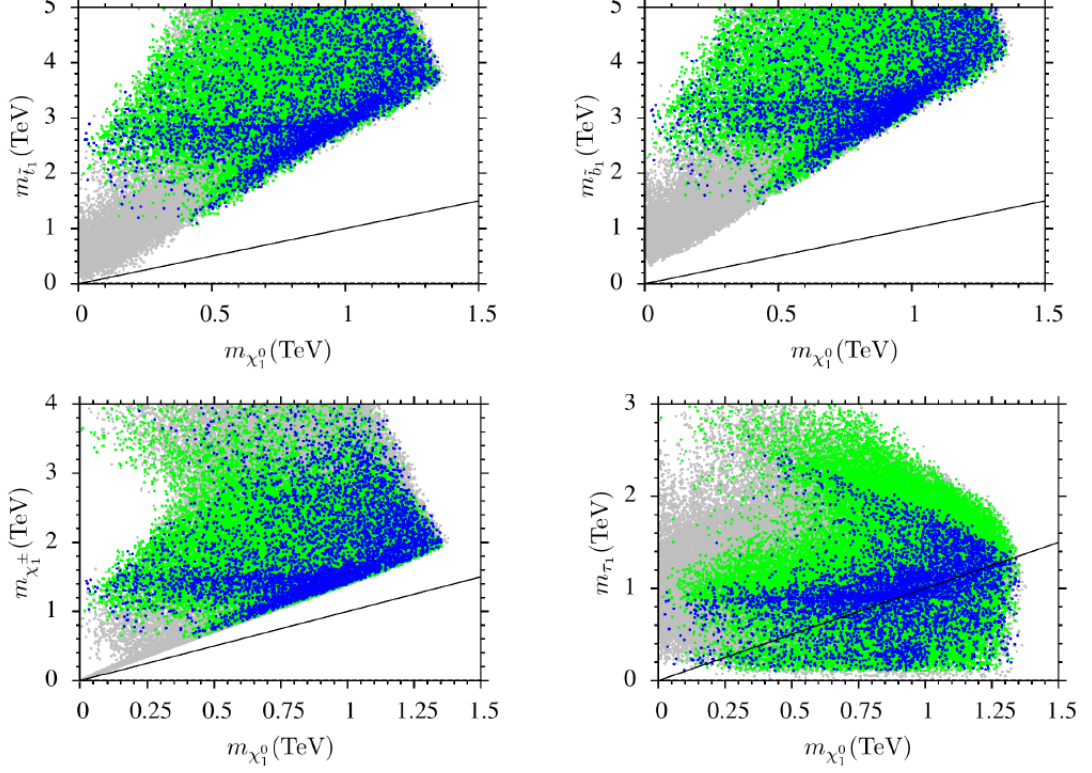


Figure 5.3. Plots in  $m_{\tilde{t}_1} - m_{\tilde{\chi}_1^0}$ ,  $m_{\tilde{b}_1} - m_{\tilde{\chi}_1^0}$ ,  $m_{\tilde{\tau}_1} - m_{\tilde{\chi}_1^0}$ , and  $m_{\tilde{\chi}_1^\pm} - m_{\tilde{\chi}_1^0}$  planes. The color coding is the same as Figure 5.1. In addition, the solid line shows the degenerate mass region in each plane.

$m_{\tilde{\chi}_1}$  and  $m_N$  reduce the singlet Higgs boson mass. The results in the  $m_0 - M_{1/2}$  plane represents that the highest values of  $m_0$  can be obtained when  $m_0 \approx M_{1/2} \sim 2$  TeV. On the other hand, one needs to consider the effects of the tri-linear scalar interaction coupling to clarify the shape of the BLSSM parameter space. The regions with larger  $m_0$  values requires positive SSB trilinear scalar interaction term. Besides, when  $A_0/m_0 \gtrsim 1.5$ ,  $m_0$  can be as large as 2 TeV and the solutions can still yield two Higgs boson with mass  $\leq 150$  GeV. When  $A_0$  is negative, the RGE evolution of  $A_N$  has an increasing slope, and its contribution to the singlet Higgs boson decreases the heavy gaugino effect. Therefore, the solutions with large  $A_N$  needs to be restricted with the low  $m_0$  and  $M_{1/2}$  values. The  $m_0 - \tan \beta$  plane shows that it is possible to find solutions with  $m_{h_2} \leq 150$  GeV for almost all values of  $\tan \beta$ . Finally the  $g_{YB}(\text{GUT}) - g_{YB}(\text{SUSY})$  plane represents our results based on the gauge kinetic mixing. Even though we vary it in the perturbative level at the GUT scale, its low scale value is found in the range  $(-0.15 - 0)$ .

In Figure 5.2 we present our results in the  $M_{\text{SUSY}} - v_X$ ,  $m_{N_2} - m_{N_1}$ ,  $M_{\tilde{N}_1} - v_X$ ,

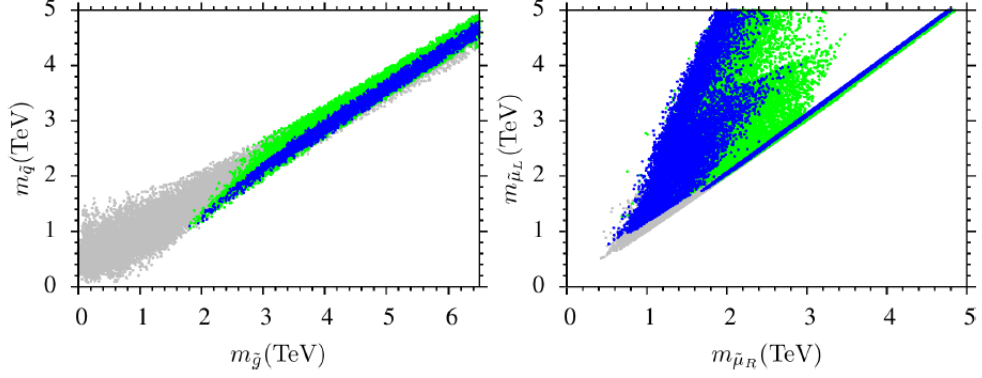


Figure 5.4. Plots in  $m_{\tilde{q}} - m_{\tilde{g}}$  and  $m_{\tilde{\mu}_L} - m_{\tilde{\mu}_R}$  planes. The color coding is the same as Figure 5.1.

and  $m_{\tilde{N}_2} - m_{\tilde{N}_1}$  planes. The color coding is the same as Figure 5.1. The solid line in the  $M_{\text{SUSY}} - v_X$  plane indicates the regions where  $M_{\text{SUSY}} = v_X$ . According to our results, the breaking of  $U(1)_{B-L}$  happens at about  $v_X \approx 5$  TeV. Since  $U(1)_{B-L}$  is no more the symmetry in the model, the existence of the right-handed neutrinos can trigger baryon and lepton number violating processes, which can be considered as a source for the baryon asymmetry in the Universe. Assuming that the supersymmetric particles all decouple below  $M_{\text{SUSY}}$ , the  $M_{\text{SUSY}} - v_X$  plane shows that  $U(1)_{B-L}$  symmetry breaking can be realized in both supersymmetric regime ( $v_X > M_{\text{SUSY}}$ ) and non-supersymmetric regime ( $v_X < M_{\text{SUSY}}$ ). In the non-supersymmetric regime, the baryon and lepton violating processes depend on the right-handed neutrinos. Since the Yukawa coupling associated with the neutrinos is very small ( $Y_\nu \sim 10^{-7}$ ), the thermal leptogenesis can provide sufficient baryon asymmetry when the right-handed neutrinos are degenerate in mass [31, 47]. As shown in the  $m_{\tilde{N}_2} - m_{\tilde{N}_1}$  plane, the right-handed neutrino masses ( $\sim 1.7 - 2.2$  TeV) are nearly degenerate. In addition to the right-handed neutrinos, the sneutrino-antisneutrino can be counted as another source in the supersymmetric regime [48]. After the right-handed neutrinos decouple,  $B - L$  symmetry is restored as a global symmetry.

Figure 5.3 represents the results for the sparticle mass spectrum with plots in  $m_{\tilde{t}_1} - m_{\tilde{\chi}_1^0}$ ,  $m_{\tilde{b}_1} - m_{\tilde{\chi}_1^0}$ ,  $m_{\tilde{\chi}_1^\pm} - m_{\tilde{\chi}_1^0}$  and  $m_{\tilde{\tau}_1} - m_{\tilde{\chi}_1^0}$  planes. The color coding is the same as Figure 5.1. In addition, the solid line shows the degenerate mass region in each plane. As is seen from the  $m_{\tilde{t}_1} - m_{\tilde{\chi}_1^0}$  and  $m_{\tilde{b}_1} - m_{\tilde{\chi}_1^0}$  planes,  $m_{\tilde{t}_1} \gtrsim 1$  and  $m_{\tilde{b}_1} \gtrsim 1.5$  TeV, and these masses are mostly required to realize the SM-like Higgs boson mass at about 125 GeV. Moreover, the  $m_{\tilde{\chi}_1^\pm} - m_{\tilde{\chi}_1^0}$  plane shows that the lightest chargino cannot be lighter than 600 GeV. Even though we do not require the neutralino to be LSP, it is found much

lighter than other sparticles except stau. The  $m_{\tilde{\tau}_1} - m_{\tilde{\chi}_1^0}$  plane represents the stau mass along with the neutralino mass, and it can be lighter than neutralino as well as being much heavier. One can constrain the stau mass further by the prompt decay of stau to gravitino in the case of gravitino LSP [49].

We continue with Figure 5.4 to present our results for the sparticle spectrum with plots in  $m_{\tilde{q}} - m_{\tilde{g}}$  and  $m_{\tilde{\mu}_L} - m_{\tilde{\mu}_R}$  planes. The color coding is the same as Figure 5.1. The  $m_{\tilde{q}} - m_{\tilde{g}}$  shows that the squarks from the first two families and gluino should be heavier than 2 TeV. Even though we impose a mass bound on gluino at about 1.8 TeV, the other LHC results mentioned in Section 5.1 constrain gluino mass further to about 2 TeV (green). Imposing the condition that  $m_{h_2} \leq 150$  GeV (blue) does not constrain the gluino or squark masses strictly. Similarly the results for the smuon masses are represented in the  $m_{\tilde{\mu}_L} - m_{\tilde{\mu}_R}$  plane. According to our results, the lightest left- and right-handed smuon masses are about 1 TeV. In this case, one can expect relatively better result for the muon anomalous magnetic moment (muon  $g - 2$ ), but since the supersymmetric contributions are more or less suppressed by the smuon masses, the results for the muon  $g - 2$  hardly reach to  $2\sigma$  band of the experimental results.

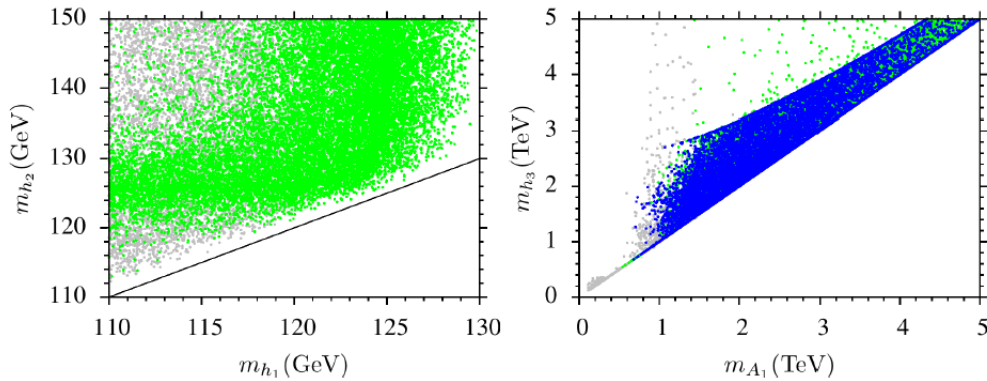


Figure 5.5. Plots in  $m_{h_2} - m_{h_1}$  and  $m_{h_3} - m_{A_1}$  planes. The color coding is the same as Figure 5.1 except that the Higgs mass bound in green is not applied in the  $m_{h_2} - m_{h_1}$  plane since  $m_{h_1}$  is plotted in one axis. The diagonal line represents the mass degeneracy.

Finally we display our results for the mass spectrum of the Higgs bosons in Figure 5.5 with plots in  $m_{h_2} - m_{h_1}$  and  $m_{h_3} - m_{A_1}$  planes. The color coding is the same as Figure 5.1 except that the Higgs mass bound in green is not applied in the  $m_{h_2} - m_{h_1}$  since  $m_{h_1}$  is plotted in one axis. The diagonal line represents the mass degeneracy. The  $m_{h_2} - m_{h_1}$  plane shows that there are plenty of solutions with  $m_{h_1}, m_{h_2} \leq 150$  GeV. Moreover,



following the diagonal line we can see that it is also possible to find the lightest two Higgs boson with almost degenerate at about  $m_{h_1} \approx m_{h_2} \sim 125$  GeV. The other Higgs bosons are found rather heavy ( $\gtrsim 1$  TeV) as shown in the  $m_{h_3} - m_{A_1}$  plane.

### 5.3. Higgs Boson Decays

We have represented the mass spectrum in BLSSM in the previous section. As mentioned, BLSSM provides an extra Higgs boson which can be lighter than 150 GeV, and even two Higgs bosons can be degenerate at about 125 GeV. With the mixing between two Higgs fields this region can provide a relatively rich phenomenology for the Higgs decays. In this section, we present our results for the Higgs decays into two photons and four leptons.

#### 5.3.1. $h \rightarrow \gamma\gamma$

The sparticles shown in Figure 5.3 contribute to the loop induced coupling between the Higgs boson and two photons in SUSY models. Since their contributions are inversely proportional to their masses, the contributions from stop and sbottom are suppressed by their heavy masses. The main contribution comes from the stau, since its mass can be as low as 100 GeV. In addition, chargino contribution can be counted as a correction. Moreover, since the second Higgs boson mass lighter than 150 GeV can be realized, there is also an induced coupling between  $h_2$  and two photons. One can quantify the excess relative to the SM prediction in  $h \rightarrow \gamma\gamma$  with the parameter  $R_{\gamma\gamma}^i$  defined as

$$R_{\gamma\gamma}^i = \frac{\sigma(pp \rightarrow h_i) \times \text{BR}(h_i \rightarrow \gamma\gamma)}{\sigma(pp \rightarrow h)_{\text{SM}} \times \text{BR}(h \rightarrow \gamma\gamma)_{\text{SM}}} \quad (5.10)$$

where  $\sigma(pp \rightarrow h_i)$  denotes the production cross-section of the Higgs boson  $h_i$ , and  $\text{BR}(h_i \rightarrow \gamma\gamma)$  is the branching ratio of the process in which the Higgs boson decays into two photons. The definitions for the terms in the denominator are the same, but they represent the SM predictions for the same process.

Eq.(5.10) reveals the importance of the Higgs boson production at the LHC as well as the loop induced coupling between the Higgs bosons and photons. Since the Higgs boson couplings to the matter fields in the first two families are negligible, the main contributions to  $\sigma(pp \rightarrow h_i)$  come from gluon fusion (GGF), vector boson fusion (VBF), associated vector boson-Higgs (VH) production and higgs production along with



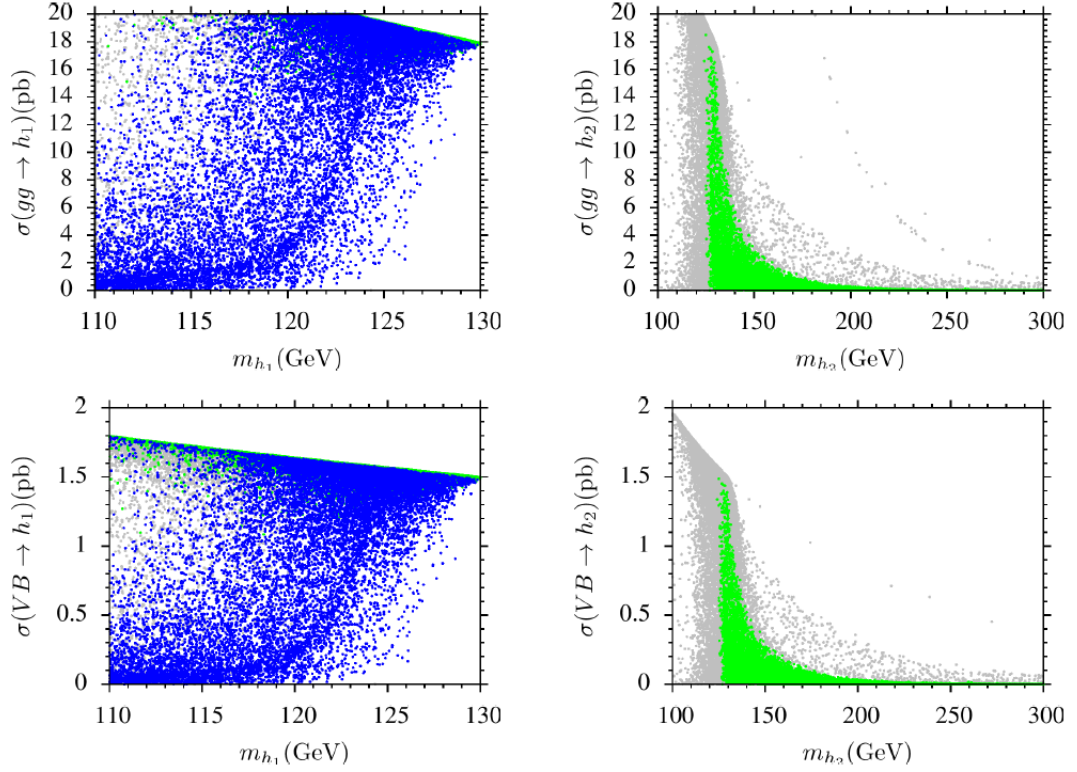


Figure 5.6. Plots for the Higgs boson production cross-section through GGF (top panel) and VBF (bottom panel) in the  $\sigma(gg \rightarrow h_1) - m_{h_1}$ ,  $\sigma(VB \rightarrow h_1) - m_{h_1}$ ,  $\sigma(gg \rightarrow h_2) - m_{h_2}$  and  $\sigma(VB \rightarrow h_2) - m_{h_2}$  planes. The color coding is the same as Figure 5.1, except we do not apply the SM Higgs boson constraint ( $m_{h_1} \sim 125$  GeV) to the left panel, since  $m_{h_1}$  is directly plotted here. Similarly, the condition  $m_{h_2} \leq 150$  GeV, represented by the blue region, is not applied to the right panels, since  $m_{h_2}$  is on the horizontal axis.

the top quark pair (ttH). Figure 5.6 displays plots for the Higgs boson production cross-section through GGF (top panel) and VBF (bottom panel) in the  $\sigma(gg \rightarrow h_1) - m_{h_1}$ ,  $\sigma(VB \rightarrow h_1) - m_{h_1}$ ,  $\sigma(gg \rightarrow h_2) - m_{h_2}$  and  $\sigma(VB \rightarrow h_2) - m_{h_2}$  planes. The color coding is the same as Figure 5.1, except we do not apply the SM Higgs boson constraint ( $m_{h_1} \sim 125$  GeV) to the left panel, since  $m_{h_1}$  is directly plotted here. Similarly, the condition  $m_{h_2} \leq 150$  GeV, represented by the blue region, is not applied to the right panels, since  $m_{h_2}$  is on the horizontal axis. As seen from the plots of Figure 5.6, GGF dominates in the Higgs boson production at the LHC as happened for the SM Higgs boson. However, while GGF yields a production cross-section of the order about  $10^2$  pb in the SM [50] and MSSM [51], in BLSSM the GGF cross-section is found at about 20 pb at most. This is because the Higgs boson couplings are diminished by  $\sin \alpha$  and  $\cos \alpha$ , where

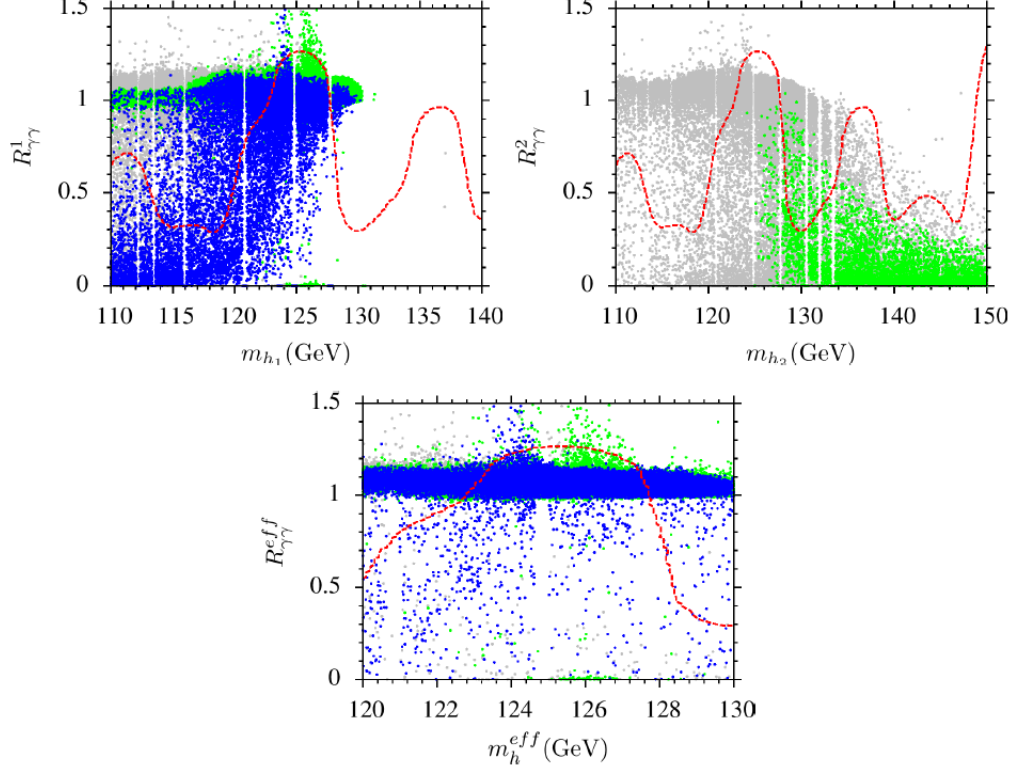


Figure 5.7. Plots in  $R_{\gamma\gamma}^1 - m_{h_1}$ ,  $R_{\gamma\gamma}^2 - m_{h_2}$  and  $R_{\gamma\gamma}^{\text{eff}} - m_h^{\text{eff}}$  planes. The color coding is the same as Figure 5.6. The red dashed line indicates the observed cross-section in  $h \rightarrow \gamma\gamma$  normalized to the SM prediction.

$\alpha$  measures the mixing between the Higgs fields. As shown in the  $\sigma(gg \rightarrow h_1) - m_{h_1}$  plane,  $h_1$  behaves mostly like the SM Higgs boson, while  $h_2$  can share this behavior when  $m_{h_2} \lesssim 150$  GeV. As seen from the  $\sigma(gg \rightarrow h_2) - m_{h_2}$  plane, the  $h_2$  production has a sharp fall for relatively heavier mass scales, and finally it drops to zero for  $m_{h_2} \gtrsim 200$  GeV. It is because the second lightest higgs boson is mostly formed by the BLSSM Higgs fields, which are SM-singlets, as the mass difference between the two lightest Higgs bosons increases. A similar discussion can hold for the VBF as shown in the bottom plane of Figure 5.6. VBF is usually the production channel with the second larger contribution, and it is one order of magnitude smaller than the GGF results.

We present our results for the possible excesses in  $h_i \rightarrow \gamma\gamma$  with plots in  $R_{\gamma\gamma}^1 - m_{h_1}$ ,  $R_{\gamma\gamma}^2 - m_{h_2}$  and  $R_{\gamma\gamma}^{\text{eff}} - m_h^{\text{eff}}$  planes. The color coding is the same as Figure 5.6. The red dashed line indicates the observed cross-section in  $h \rightarrow \gamma\gamma$  normalized to the SM prediction. As seen from the  $R_{\gamma\gamma}^1 - m_{h_1}$  plane, BLSSM yields plenty of solutions which can feed the excess in  $h \rightarrow \gamma\gamma$  for both  $m_{h_2} \leq 150$  GeV (blue) and  $m_{h_2} \geq 150$

GeV (green). These solutions can be explained by effects of the light staus and relatively light charginos as shown in Figure 5.3. In addition to the light sparticles, also the second lightest Higgs boson mass can be realized as nearly degenerate with  $m_{h_1} \approx 125$  GeV, and it can be seen from the  $R_{\gamma\gamma}^2 - m_{h_2}$  plane that it can provide some cross-section in  $h \rightarrow \gamma\gamma$  as much as the SM ( $R_{\gamma\gamma}^2 \sim 1$ ). In this region, we have two Higgs bosons of mass about 125 GeV, and both contribute to the cross-section of  $h \rightarrow \gamma\gamma$ . If we define  $m_h^{\text{eff}}$  and  $R_{\gamma\gamma}^{\text{eff}}$  as

$$m_h^{\text{eff}} = \frac{m_{h_1} R_{\gamma\gamma}^1 + m_{h_2} R_{\gamma\gamma}^2}{R_{\gamma\gamma}^1 + R_{\gamma\gamma}^2}, \quad R_{\gamma\gamma}^{\text{eff}} = R_{\gamma\gamma}^1 + R_{\gamma\gamma}^2 \quad (5.11)$$

the predicted effective cross-section by many solutions are lifted up to region where  $R_{\gamma\gamma}^{\text{eff}} \gtrsim 1$  for  $m_h^{\text{eff}} \sim 125$  GeV, as seen from the  $R_{\gamma\gamma}^{\text{eff}} - m_h^{\text{eff}}$  plane.

Before concluding it should be noted that the second lightest higgs boson can be accounted for the other peaks at about 137 GeV and 145 GeV observed in the experiments. As seen from the  $R_{\gamma\gamma}^2 - m_{h_2}$  panel, the solutions may relatively provide some non-zero cross-sections at these mass scales. However, the solutions around the second peak at 137 GeV are excluded by the Higgs boson constraint. Since we have restricted ourselves with the universal boundary conditions at  $M_{\text{GUT}}$ , these predictions can be ameliorated by imposing non-universality.

### 5.3.2. $h \rightarrow 4l$

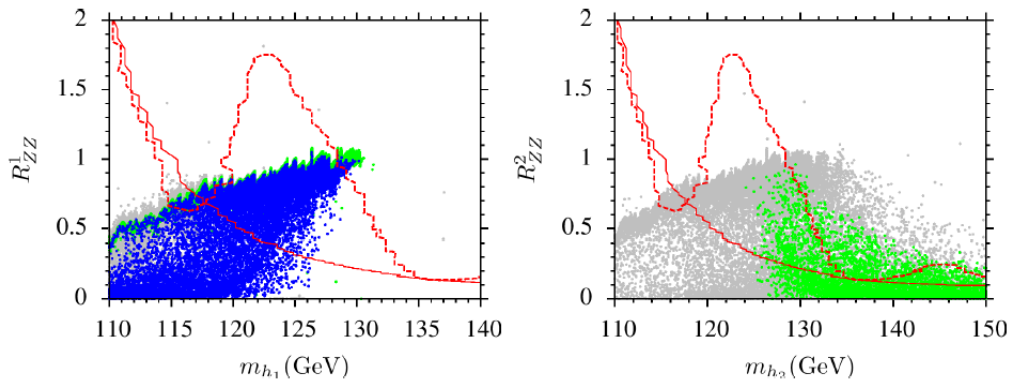


Figure 5.8. Plots in  $R_{ZZ}^1 - m_{h_1}$  and  $R_{ZZ}^2 - m_{h_2}$ . The color coding is the same as Figure 5.6. The dashed line indicates the observed cross-section, while the solid line represents the expected cross-section without the Higgs boson.

A similar discussion can be followed for the process in which the Higgs boson decays into four leptons. In the SM, this process is mediated via two  $Z$ -bosons, each of which eventually decays into a lepton pair. In BLSSM, such decays can include also  $Z'$ , but due to its heavy mass ( $m_{Z'} = 2.5$  TeV in our work), such processes are highly suppressed. Hence, the difference in  $h \rightarrow 4l$  between BLSSM and the observation basically come from the Higgs boson decays into two  $Z$ -bosons. Figure 5.8 represents our results with plots in  $R_{ZZ}^1 - m_{h_1}$  and  $R_{ZZ}^2 - m_{h_2}$ . The color coding is the same as Figure 5.6. The dashed line indicates the observed cross-section, while the solid line represents the expected cross-section without the Higgs boson. In contrast to the Higgs decays into two photons, BLSSM's predictions can be only as good as ones in the SM, even in the case of the degenerate Higgs bosons. On the other hand, if one considers the second peak observed at  $m_h \sim 145$  GeV, it can be seen from the  $R_{ZZ}^2 - m_{h_2}$  plane, the second Higgs boson can nicely fill the region around this peak.

## CHAPTER 6

### CONCLUSION

We presented the predictions on the mass spectrum and Higgs boson decays in the BLSSM framework with universal boundary conditions. We briefly mentioned about the right-handed neutrino sector. The radiative breaking of  $U(1)_{B-L}$  symmetry happens at about 5 TeV below which  $B-L$  is no more the conserved symmetry and the right-handed neutrinos can trigger baryon and lepton number violating process till they decouple from the SM sector at 1.7 – 2.2 TeV. Radiative breaking of  $B-L$  symmetry can happen in both supersymmetric ( $v_X > M_{\text{SUSY}}$ ) and non-supersymmetric ( $v_X < M_{\text{SUSY}}$ ). The sneutrino-antisneutrino mixing can be counted as another source for baryon and lepton asymmetry in the Universe.

We found the stop and sbottom masses heavier than 1.5 TeV, and gluino mass greater than 2 TeV. The color sector is required to be heavy in order to realize the SM-like Higgs boson consistent with the observations. Even though BLSSM's predictions for the Higgs boson are similar to MSSM, it predicts another Higgs boson, which can be lighter than 150 GeV, and even degenerate with the lightest CP-even Higgs boson at about 125 GeV. Besides light staus ( $\gtrsim 100$  GeV), the second Higgs boson also contributes to the Higgs decay processes in the presence of gauge kinetic mixing. We showed that the excess in  $h \rightarrow \gamma\gamma$  at about 125 GeV mass scale can be realized. The solutions which can provide an excess at 137 GeV and 145 GeV in this process are rather excluded by the 125 GeV Higgs boson constraint. Such solutions can be improved by considering non-universal boundary conditions in BLSSM. In addition, we concluded that the BLSSM predictions for  $h \rightarrow 4l$  are only as good as the ones of the SM, but it is eligible to fit the second excess at about 145 GeV.

## REFERENCES

- [1] C. S. Ün and Ö. Özdal, Phys. Rev. D **93**, 5 (2016) [arXiv:1601.02494 [hep-ph]].
- [2] Peter W. Higgs, Phys. Rev. Lett. **13**, 10 (1964).
- [3] G. Aad *et al.* [ATLAS Collaboration], Phys. Lett. B **716**, 1 (2012).
- [4] S. Chatrchyan *et al.* [CMS Collaboration], Phys. Lett. B **716**, 30 (2012).
- [5] L. H. Ryder. Quantum Field Theory (Cambridge University Press, Cambridge 1985).
- [6] C. Burgess and G. Moore, "The Standard Model: A Primer," Cambridge (2012) 560 p
- [7] Langacker, P. ,2009. Introduction to the Standard Model and Electroweak Physics arXiv:0901.0241 [hep-ph].
- [8] Novaes, S. F. "Standard model: An Introduction," arXiv:hep-ph/0001283.
- [9] E. Gildener, Phys. Rev. D **14**, 1667 (1976); E. Gildener, Phys. Lett. B **92**, 111 (1980); S. Weinberg, Phys. Lett. B **82**, 387 (1979); L. Susskind, Phys. Rev. D **20**, 2619 (1979); M. J. G. Veltman, Acta Phys. Polon. B **12**, 437 (1981);
- [10] G. Degrassi, S. Di Vita, J. Elias-Miro, J. R. Espinosa, G. F. Giudice, G. Isidori and A. Strumia, JHEP **1208**, 098 (2012) [arXiv:1205.6497 [hep-ph]]; F. Bezrukov, M. Y. Kalmykov, B. A. Kniehl and M. Shaposhnikov, JHEP **1210**, 140 (2012) [arXiv:1205.2893 [hep-ph]]; D. Buttazzo, G. Degrassi, P. P. Giardino, G. F. Giudice, F. Sala, A. Salvio and A. Strumia, JHEP **1312**, 089 (2013) [arXiv:1307.3536].
- [11] V. Khachatryan *et al.* [CMS Collaboration], arXiv:1504.00936 [hep-ex].
- [12] [CMS Collaboration], CMS-PAS-HIG-13-001.
- [13] S. Chatrchyan *et al.* [CMS Collaboration], Phys. Rev. D **89**, no. 9, 092007 (2014) [arXiv:1312.5353 [hep-ex]].

- [14] For an incomplete list, see  
P. M. Ferreira, R. Santos, H. E. Haber and J. P. Silva, Phys. Rev. D **87**, 055009 (2013) [arXiv:1211.3131 [hep-ph]]; T. Han, T. Li, S. Su and L. T. Wang, JHEP **1311**, 053 (2013) [arXiv:1306.3229 [hep-ph]]; J. Ke, H. Luo, M. x. Luo, K. Wang, L. Wang and G. Zhu, Phys. Lett. B **723**, 113 (2013) [arXiv:1211.2427 [hep-ph]].
- [15] M. Carena, S. Gori, I. Low, N. R. Shah and C. E. M. Wagner, JHEP **1302**, 114 (2013) [arXiv:1211.6136 [hep-ph]].
- [16] D. A. Demir and C. S. Ün, Phys. Rev. D **90**, 095015 (2014) [arXiv:1407.1481 [hep-ph]].
- [17] I. Gogoladze, F. Nasir and Q. Shafi, JHEP **1311**, 173 (2013) [arXiv:1306.5699 [hep-ph]].
- [18] R. Aaij *et al.* [LHCb Collaboration], Phys. Rev. Lett. **110**, no. 2, 021801 (2013) [arXiv:1211.2674 [hep-ex]].
- [19] C. Bobeth, M. Gorbahn, T. Hermann, M. Misiak, E. Stamou and M. Steinhauser, Phys. Rev. Lett. **112**, 101801 (2014) [arXiv:1311.0903 [hep-ph]]; C. Bobeth, M. Gorbahn and E. Stamou, Phys. Rev. D **89**, no. 3, 034023 (2014) [arXiv:1311.1348 [hep-ph]]; T. Hermann, M. Misiak and M. Steinhauser, JHEP **1312**, 097 (2013) [arXiv:1311.1347 [hep-ph]].
- [20] I. Gogoladze, B. He, A. Mustafayev, S. Raza and Q. Shafi, JHEP **1405**, 078 (2014) [arXiv:1401.8251 [hep-ph]].
- [21] P. Langacker, Rev. Mod. Phys. **81**, 1199 (2009) [arXiv:0801.1345 [hep-ph]] and references therein.
- [22] R. Wendell *et al.* [Super-Kamiokande Collaboration], Phys. Rev. D **81**, 092004 (2010) [arXiv:1002.3471 [hep-ex]].
- [23] C. S. Aulakh, A. Melfo, A. Rasin and G. Senjanovic, Phys. Lett. B **459**, 557 (1999) doi:10.1016/S0370-2693(99)00708-X [hep-ph/9902409].
- [24] M. Adeel Ajaib, I. Gogoladze and Q. Shafi, Phys. Rev. D **91**, no. 9, 095005 (2015)

- [arXiv:1501.04125 [hep-ph]].
- [25] S. Khalil and A. Masiero, Phys. Lett. B **665**, 374 (2008) [arXiv:0710.3525 [hep-ph]].
- [26] J. E. Camargo-Molina, B. O’Leary, W. Porod and F. Staub, PoS EPS -**HEP2013**, 265 (2013) [arXiv:1310.1260 [hep-ph]].
- [27] S. Khalil and C. S. Un, arXiv:1509.05391 [hep-ph].
- [28] B. Holdom, Phys. Lett. B **166**, 196 (1986); K. S. Babu, C. F. Kolda and J. March-Russell, Phys. Rev. D **57**, 6788 (1998) [hep-ph/9710441]; F. del Aguila, G. D. Coughlan and M. Quiros, Nucl. Phys. B **307**, 633 (1988) [Nucl. Phys. B **312**, 751 (1989)]; F. del Aguila, J. A. Gonzalez and M. Quiros, Nucl. Phys. B **307**, 571 (1988); R. Foot and X. G. He, Phys. Lett. B **267**, 509 (1991); T. Matsuoka and D. Suematsu, Prog. Theor. Phys. **76**, 901 (1986).
- [29] B. O’Leary, W. Porod and F. Staub, JHEP **1205**, 042 (2012) [arXiv:1112.4600 [hep-ph]].
- [30] P. H. Chankowski, S. Pokorski and J. Wagner, Eur. Phys. J. C **47**, 187 (2006) [hep-ph/0601097].  
M. Abbas and S. Khalil, JHEP **0804**, 056 (2008) doi:10.1088/1126-6708/2008/04/056 [arXiv:0707.0841 [hep-ph]].
- [31] M. Abbas and S. Khalil, JHEP **0804**, 056 (2008) [arXiv:0707.0841 [hep-ph]].
- [32] R. N. Mohapatra and J. W. F. Valle, Phys. Rev. D **34**, 1642 (1986); M. C. Gonzalez-Garcia and J. W. F. Valle, Phys. Lett. B **216**, 360 (1989); S. Khalil, Phys. Rev. D **82**, 077702 (2010) [arXiv:1004.0013 [hep-ph]].
- [33] A. Elsayed, S. Khalil and S. Moretti, Phys. Lett. B **715**, 208 (2012) [arXiv:1106.2130 [hep-ph]]; S. Khalil, Phys. Rev. D **82**, 077702 (2010) [arXiv:1004.0013 [hep-ph]].
- [34] W. Porod, Comput. Phys. Commun. **153**, 275 (2003) [hep-ph/0301101];  
W. Porod and F. Staub, Comput. Phys. Commun. **183**, 2458 (2012) doi:10.1016/j.cpc.2012.05.021 [arXiv:1104.1573 [hep-ph]].



- [35] F. Staub, arXiv:0806.0538 [hep-ph]; F. Staub, *Comput. Phys. Commun.* **182**, 808 (2011) [arXiv:1002.0840 [hep-ph]].
- [36] J. Hisano, H. Murayama and T. Yanagida, *Nucl. Phys. B* **402**, 46 (1993) [hep-ph/9207279]; Y. Yamada, *Z. Phys. C* **60**, 83 (1993); J. L. Chkareuli and I. G. Gogoladze, *Phys. Rev. D* **58**, 055011 (1998) [hep-ph/9803335].
- [37] L. E. Ibanez and G. G. Ross, *Phys. Lett.* **B110** (1982) 215; K. Inoue, A. Kakuto, H. Komatsu and S. Takeshita, *Prog. Theor. Phys.* **68**, 927 (1982) [Erratum-ibid. **70**, 330 (1983)]; L. E. Ibanez, *Phys. Lett.* **B118** (1982) 73; J. R. Ellis, D. V. Nanopoulos, and K. Tamvakis, *Phys. Lett.* **B121** (1983) 123; L. Alvarez-Gaume, J. Polchinski, and M. B. Wise, *Nucl. Phys.* **B221** (1983) 495.
- [38] T. E. W. Group [CDF and D0 Collaborations], arXiv:0903.2503 [hep-ex].
- [39] I. Gogoladze, R. Khalid, S. Raza and Q. Shafi, *JHEP* **1106**, 117 (2011) doi:10.1007/JHEP06(2011)117 [arXiv:1102.0013 [hep-ph]].
- [40] I. Gogoladze, Q. Shafi and C. S. Un, *JHEP* **1208**, 028 (2012) doi:10.1007/JHEP08(2012)028 [arXiv:1112.2206 [hep-ph]]; M. Adeel Ajaib, I. Gogoladze, Q. Shafi and C. S. Un, *JHEP* **1307**, 139 (2013) doi:10.1007/JHEP07(2013)139 [arXiv:1303.6964 [hep-ph]].
- [41] G. Belanger, F. Boudjema, A. Pukhov and R. K. Singh, *JHEP* **0911**, 026 (2009); H. Baer, S. Kraml, S. Sekmen and H. Summy, *JHEP* **0803**, 056 (2008).
- [42] K. A. Olive *et al.* [Particle Data Group Collaboration], *Chin. Phys. C* **38**, 090001 (2014). doi:10.1088/1674-1137/38/9/090001
- [43] Y. Amhis *et al.* [Heavy Flavor Averaging Group Collaboration], arXiv:1207.1158 [hep-ex].
- [44] D. Asner *et al.* [Heavy Flavor Averaging Group Collaboration], arXiv:1010.1589 [hep-ex].
- [45] M. Davier, A. Hoecker, B. Malaescu and Z. Zhang, *Eur. Phys. J. C* **71**, 1515 (2011) [*Eur. Phys. J. C* **72**, 1874 (2012)] [arXiv:1010.4180 [hep-ph]]; K. Hagiwara,

R. Liao, A. D. Martin, D. Nomura and T. Teubner, *J. Phys. G* **38**, 085003 (2011) [arXiv:1105.3149 [hep-ph]].

[46] See for instance;

H. Baer, I. Gogoladze, A. Mustafayev, S. Raza and Q. Shafi, *JHEP* **1203**, 047 (2012) doi:10.1007/JHEP03(2012)047 [arXiv:1201.4412 [hep-ph]]; T. Li, D. V. Nanopoulos, S. Raza and X. C. Wang, *JHEP* **1408**, 128 (2014) doi:10.1007/JHEP08(2014)128 [arXiv:1406.5574 [hep-ph]].

[47] M. Flanz, E. A. Paschos and U. Sarkar, *Phys. Lett. B* **345**, 248 (1995) [*Phys. Lett. B* **382**, 447 (1996)] doi:10.1016/0370-2693(94)01555-Q [hep-ph/9411366]; M. Flanz, E. A. Paschos, U. Sarkar and J. Weiss, *Phys. Lett. B* **389**, 693 (1996) doi:10.1016/S0370-2693(96)01337-8 [hep-ph/9607310]; L. Covi, E. Roulet and F. Vissani, *Phys. Lett. B* **384**, 169 (1996) doi:10.1016/0370-2693(96)00817-9 [hep-ph/9605319]; A. Pilaftsis, *Phys. Rev. D* **56**, 5431 (1997) doi:10.1103/PhysRevD.56.5431 [hep-ph/9707235];

[48] Y. Grossman, T. Kashti, Y. Nir and E. Roulet, *Phys. Rev. Lett.* **91**, 251801 (2003) doi:10.1103/PhysRevLett.91.251801 [hep-ph/0307081]; E. J. Chun, *Phys. Rev. D* **69**, 117303 (2004) doi:10.1103/PhysRevD.69.117303 [hep-ph/0404029]; Y. Grossman, T. Kashti, Y. Nir and E. Roulet, *JHEP* **0411**, 080 (2004) doi:10.1088/1126-6708/2004/11/080 [hep-ph/0407063]; Y. Grossman, R. Kitano and H. Murayama, *JHEP* **0506**, 058 (2005) doi:10.1088/1126-6708/2005/06/058 [hep-ph/0504160]; Y. Kajiyama, S. Khalil and M. Raidal, *Nucl. Phys. B* **820**, 75 (2009) doi:10.1016/j.nuclphysb.2009.05.011 [arXiv:0902.4405 [hep-ph]].

[49] L. Calibbi, A. Mariotti, C. Petersson and D. Redigolo, *JHEP* **1409**, 133 (2014) doi:10.1007/JHEP09(2014)133 [arXiv:1405.4859 [hep-ph]]; I. Gogoladze, Q. Shafi and C. S. Ün, *Phys. Rev. D* **92**, no. 11, 115014 (2015) doi:10.1103/PhysRevD.92.115014 [arXiv:1509.07906 [hep-ph]].

[50] A. Djouadi, *Phys. Rept.* **457**, 1 (2008) doi:10.1016/j.physrep.2007.10.004 [hep-ph/0503172].

[51] A. Djouadi, *Phys. Rept.* **459**, 1 (2008) doi:10.1016/j.physrep.2007.10.005 [hep-ph/0503173].